Strengthening Of RC Beam Using FRP Sheet

E. Rakesh Reddy[1], G. Ramakrishna[2]

Abstract: *Strengthening structures via external bonding of advanced fibre reinforced polymer (FRP) composite is becoming very popular worldwide during the past decade because it provides a more economical and technically superior alternative to the traditional techniques in many situations as it offers high strength, low weight, corrosion resistance, high fatigue resistance, easy and rapid installation and minimal change in structural geometry. Although many in-situ RC beams are continuous in construction, there has been very limited research work in the area of FRP strengthening of continuous beams. In the present study an experimental investigation is carried out to study the behavior of continuous RC beams under static loading. The beams are strengthened with externally bonded glass fibre reinforced polymer (GFRP) sheets. Different scheme of strengthening have been employed. The program consists of fourteen continuous (two-span) beams with overall dimensions equal to (150×200×2300) mm. The beams are grouped into two series labeled S1 and S2 and each series have different percentage of steel reinforcement. One beam from each series (S1 and S2) was not strengthened and was considered as a control beam, whereas all other beams from both the series were strengthened in various patterns with externally bonded GFRP sheets. The present study examines the responses of RC continuous beams, in terms of failure modes, enhancement of load capacity and load deflection analysis. The results indicate that the flexural strength of RC beams can be significantly increased by gluing GFRP sheets to the tension face. In addition, the epoxy bonded sheets improved the cracking behaviour of the beams by delaying the formation of visible cracks and reducing crack widths at higher load levels. The experimental results were validated by using finite element method.*

Keywords: *continuous beam; flexural strengthening; GFRP; premature failure; debonding failure.*

ABBREVIATIONS

ACI	American Concrete Institute
CFRP	Carbon Fibre Reinforced Polymer
BM	Bending Moment
EB	Externally Bonded
FEM	Finite Element Method
FRP	Fibre Reinforced Polymer
FRPC	Fibre Reinforced Polymer Composite
GFRP	Glass Fibre Reinforced plastic
HSC	High Strength Concrete
HYSD	High Yield Strength Deformed
IC	Intermediate Crack
IS	Indian Standards
NSM	Near Surface mounted
PSC	Portland Slag Cement
RC	Reinforced Concrete
RHSC	Reinforced High Strength Concrete

NOTATIONS

D	Overall Depth of the Beam
B	Breadth of the Beam
d	Effective Depth
L	Span Length of the Beam
fck	Characteristic Cube Compressive Strength of Concrete
fy	Tensile Strength of the Bar

Pu	Ultimate Load
λ	Load Enhancement Ratio
φ	Diameter of the Reinforcement
M	Moment of Resistance
E	Modulus of Elasticity
I	Moment of Inertia
F	Global Nodal Force Vector
K	Stiffness Matrix
U	Global Nodal Displacement Vector
u	Displacement Field
Ni	Interpolation Function
ui	Nodal Displacements

I. Introduction

1.1 General

A structure is designed for a specific period and depending on the nature of the structure, its design life varies. For a domestic building, this design life could be as low as twenty-five years, whereas for a public building, it could be fifty years. Deterioration in concrete structures is a major challenge faced by the infrastructure and bridge industries worldwide. The deterioration can be mainly due to environmental effects, which includes corrosion of steel, gradual loss of strength with ageing, repeated high intensity loading, variation in temperature, freeze-thaw cycles, contact with chemicals and saline water and exposure to ultra-violet radiations. As complete replacement or reconstruction of the structure will be cost effective, strengthening or retrofitting is an effective way to strengthen the same. The most popular techniques for strengthening of RC beams have involved the use of external epoxy-bonded steel plates. It has been found experimentally that flexural strength of a structural member can increase by using this technique. Although steel bonding technique is simple, cost-effective and efficient, it suffers from a serious problem of deterioration of bond at the steel and concrete interphase due to corrosion of steel. Other common strengthening technique involves construction of steel jackets which is quite effective from strength, stiffness and ductility considerations. However, it increases overall cross-sectional dimensions, leading to increase in self-weight of structures and is labour intensive. To eliminate these problems, steel plate was replaced by corrosion resistant and light-weight FRP Composite plates. FRPCs help to increase strength and ductility without excessive increase in stiffness. Further, such material could be designed to meet specific requirements by adjusting placement of fibres. So concrete members can now be easily and effectively strengthened using externally bonded FRP composites. By wrapping FRP sheets, retrofitting of concrete structures provide a more economical and technically superior alternative to the traditional techniques in many situations because it offers high strength, low weight, corrosion resistance, high fatigue resistance, easy and rapid installation and minimal change in structural geometry. FRP systems can also be used in areas with limited access where traditional techniques would be impractical. However, due to lack of the proper knowledge on structural behavior of concrete structures, the use of these materials for retrofitting the existing concrete structures cannot reach up to the expectation. Successful retrofitting of concrete structures with FRP needs a thorough knowledge on the subject and available user-friendly technologies/ unique guidelines.

Beams are the critical structural members subjected to bending, torsion and shear in all type of structures. Similarly, columns are also used as various important elements subjected to axial load combined with/without bending and are used in all type of structures. Therefore, extensive research works are being carried out throughout world on retrofitting of concrete beams and columns with externally bonded FRP composites. Several investigators took up concrete beams and columns retrofitted with carbon fibre reinforced polymer (CFRP)/ glass fibre reinforced polymer (GFRP) composites in order to study the enhancement of strength and ductility, durability, effect of confinement, preparation of design guidelines and experimental investigations of these members.

1.2 Flexural Strenghtening of Beams

For flexural strengthening, there are many methods such as: section enlargement, steel plate bonding, external post tensioning method, near-surface mounted (NSM) system and externally bonded (EB) system. While many methods of strengthening structures are available, strengthening structures via external bonding of advanced fibre-reinforced polymer composite (FRP) has become very popular worldwide. During the past decade, their application in this field has been rising due to the well-known advantages of FRP composites over other materials. Consequently, a great quantity of research, both experimental and theoretical, has been conducted on the behaviour of FRP-strengthened reinforced concrete (RC) structures. In this regard, the evolving technology of using carbon-bonded fibre-reinforced polymers (CFRP) for strengthening of RC beams has attracted much attention in recent years.

1.3 Advantages of FRP
Some of the main advantages of FRP can be listed below:

Low weight: The FRP is much less dense and therefore lighter than the equivalent volume ofsteel. The lower weight of FRP makes installation and handling significantly easier than steel. These properties are particularly important when installation is done in cramped locations. Other works like works on soffits of bridges and building floor slabs are carried out from man-access platforms rather than from full scaffolding. The use of fibre composites does not significantly increase the weight of the structure or the dimensions of the member. And because of their light weight, the transport of FRP materials has minimal environmental impact.

Mechanical strength: FRP can provide a maximum material stiffness to density ratio of 3.5to 5 times that of aluminium or steel. FRP is so strong and stiff for its weight, it can out-perform the other materials.

Formability: The material can take up irregularities in the shape of the concrete surface. Itcan be moulded to almost any desired shape. We can create or copy most shapes with ease.

Chemical resistance: FRP is minimally reactive, making it ideal as a protective covering forsurfaces where chemical

Joints: Laps and joints are not required.

Corrosion resistance: Unlike metal, FRP does not rust away and it can be used to make long-lasting structures.

Low maintenance: Once FRP is installed, it requires minimal maintenance. The materialsfibres and resins are durable if correctly specified, and require little maintenance. If they are damaged in service, it is relatively simple to repair them, by adding an additional layer.

Long life: It has high resistance to fatigue and has shown excellent durability over the last 50 years.

Easy to apply: The application of FRP plate or sheet material is like applying wallpaper;once it has been rolled on carefully to remove entrapped air and excess adhesive it may be left unsupported. Fibre composite materials are available in very long lengths while steel plate is generally limited to 6 m. These various factors in combination lead to a significantly simpler and quicker strengthening process than when using steel plate.

1.4 Suitability of Frp for Uses in Structural Engineering
The strength properties of FRPs collectively make up one of the primary reasons for which civil engineers select them in the design of structures. A material's strength is governed by its ability to sustain a load without excessive deformation or failure. When an FRP specimen is tested in axial tension, the applied force per unit cross-sectional area (stress) is proportional to the ratio of change in a specimen's length to its original length (strain). When the applied load is removed, FRP returns to its original shape or length. In other words, FRP responds linear-elastically to axial stress. The response of FRP to axial compression is reliant on the relative proportion in volume of fibres, the properties of the fibre and resin, and the interface bond strength. FRP composite compression failure occurs when the fibres exhibit extreme (often sudden and dramatic) lateral or sides-way deflection called fibre buckling. FRP's response to transverse tensile stress is very much dependent on the properties of the fibre and matrix, the interaction between the fibre and matrix, and the strength of the fibre-matrix interface. Generally, however, tensile strength in this direction is very poor. Shear stress is induced in the plane of an area when external loads tend to cause two segments of a body to slide over one another. The shear strength of FRP is difficult to quantify. Generally, failure will occur within the matrix material parallel to the fibres. Among FRP's high strength properties, the most relevant features include excellent durability and corrosion resistance. Furthermore, their high strength-to-weight ratio is of significant benefit; a member composed of FRP can support larger live loads since its dead weight does not contribute significantly to the loads that it must bear. Other features include ease of installation, versatility, anti-seismic behaviour, electromagnetic neutrality, excellent fatigue behaviour, and fire resistance. However, like most structural materials, FRPs have a few drawbacks that would create some hesitancy in civil engineers to use it for all applications: high cost, brittle behaviour, susceptibility to deformation under long-term loads, UV degradation, photo-degradation (from exposure to light), temperature and moisture effects, lack of design codes, and most importantly, lack of awareness.

1.5 Applications of Frp Composites in Construction
There are three broad divisions into which applications of FRP in civil engineering can be classified: applications for new construction, repair and rehabilitation applications, and architectural applications. FRPs have been used widely by civil engineers in the design of new construction. Structures such as bridges and columns built completely out of FRP composites have demonstrated exceptional durability, and effective resistance to effects of environmental exposure. Pre-stressing tendons, reinforcing bars, grid reinforcement and dowels are all examples of the many diverse applications of FRP in new structures. One of the most common uses for FRP involves the repair and rehabilitation of damaged or deteriorating structures. Several companies across the world are beginning to wrap damaged bridge piers to prevent collapse and steel-reinforced columns to

improve the structural integrity and to prevent buckling of the reinforcement. Architects have also discovered the many applications for which FRP can be used. These include structures such as siding/cladding, roofing, flooring and partitions.

1.6 Current Research on FRP
A serious matter relating to the use of FRPs in civil applications is the lack of design codes and specifications. For nearly a decade now, researchers from Canada, Europe, and Japan have been collaborating their efforts in hope of developing such documents to provide guidance for engineers designing FRP structures.

1.7 Design Considerations
The development of the advanced composite technology is an engineer's dream for innovative design and application. The characteristics of a composite can be tailored and designed to meet any desired specifications. Most of the information and design data available on composites are in the aerospace applications, but they are protected under the guise of proprietary systems and/or military classified documents. Unlike conventional isotropic materials of steel and concrete, there are no readily available design charts and guidelines to help the structural engineer. When it comes to working with composites as opposed to conventional materials, as the author has discovered, the difference can be as dramatic as night and day.

1.8 Disadvantages of Frp
The main disadvantage of externally strengthening structures with fibre composite materials is the risk of fire, vandalism or accidental damage, unless the strengthening is protected. A particular concern for bridges over roads is the risk of soffit reinforcement being hit by over-height vehicles.
A perceived disadvantage of using FRP for strengthening is the relatively high cost of the materials. However, comparisons should be made on the basis of the complete strengthening exercise; in certain cases the costs can be less than that of steel plate bonding. A disadvantage in the eyes of many clients will be the lack of experience of the techniques and suitably qualified staff to carry out the work. Finally, a significant disadvantage is the lack of accepted design standards.

II.   Review Of Literature

2.1 Brief Review
This chapter provides a review of literature on strengthening of RC concrete beams. This review comprises of literature on strengthened beam under two types of support condition i.e. simply supported and continuously supported.

2.1.1 Simply Supported Beam
Grace et al. (1999) investigated the behaviour of RC beams strengthened with CFRP and GFRP sheets and laminates. They studied the influence of the number of layers, epoxy types, and strengthening pattern on the response of the beams. They found that all beams experienced brittle failure, with appreciable enhancement in strength, thus requiring a higher factor of safety in design.

Experimental investigations, theoretical calculations and numerical simulations showed that strengthening the reinforced concrete beams with externally bonded CFRP sheets in the tension zone considerably increased the strength at bending, reduced deflections as well as cracks width (Ross et al., 1999; Sebastian, 2001; Smith & Teng, 2002; Yang et al., 2003; Aiello & Ombres, 2004). It also changed the behaviour of these beams under load and failure pattern. Most often the strengthened beams failed in a brittle way, mainly due to the loss of connection between the composite material and the concrete. The influence of the surface preparation of the concrete, adhesive type, and concrete strength on the overall bond strength is studied as well as characteristics of force transfer from the plate to concrete. They concluded that the surface preparation along with along with soundness of concrete could influence the ultimate bond strength. Thereafter, Study on de-bonding problems in concrete beams externally strengthened with FRP composites are carried out by many researchers.

Many investigators used externally bonded FRP composites to improve the flexural strength of reinforced concrete members. To evaluate the flexural performance of the strengthened members, it is necessary to study flexural stiffness of FRP strengthened members at different stages, such as pre-cracking, post-cracking and post-yielding. However, only few studied are focused on the reinforced concrete members strengthened under pre-loading or pre-cracking (Arduni & Nanni, 1997).

F. Ceroni(2010) investigated the experimental program on Reinforced Concrete (RC) beams externally strengthened with carbon Fibre Reinforced Plastic (FRP) laminates and Near Surface Mounted (NSM) bars under monotonic and cyclic loads, the latter ones characterized by a low number of cycles in the elastic and post-elastic range. Comparisons between experimental and theoretical failure loads are discussed in detail.

Obaidat et al. (2010) studied the Retrofitting of reinforced concrete beams using composite laminates

---

and the main variables considered are the internal reinforcement ratio, position of retrofitting and the length of CFRP. The experimental tests were performed to investigate the behaviour of beams designed in such a way that either flexural or shear failure will be expected. The beams were loaded in four-point bending until cracks developed. The beams were then unloaded and retrofitted with CFRP. Finally the beams were loaded until failure. The ABAQUS program was used to develop finite element models for simulation of the behaviour of beams. The concrete was modelled using a plastic damage model and two models, a perfect bond model and a cohesive model, were evaluated for the concrete-CFRP interface. From the analyses the load-deflection relationships until failure, failure modes and crack patterns were obtained and compared to the experimental results. The FEM results agreed well with the experiments when using the cohesive model regarding failure mode and load capacity while the perfect bond model was not able to represent the debonding failure mode. The results showed that when the length of CFRP increases the load capacity of the beam increases both for shear and flexural retrofitting. FEM results also showed that the width and stiffness of CFRP affect the failure mode of retrofitted beams. The maximum load increases with increased width. Increased CFRP stiffness increases the maximum load only up to a certain value of the stiffness, and thereafter it decreases the maximum load.

In another research, Hee Sun Kim (2011) carried on experimental studies of 14 reinforced concrete (RC) beams retrofitted with new hybrid fibre reinforced polymer (FRP) system consisting carbon FRP (CFRP) and glass FRP (GFRP). The objective of this study was to examine effect of hybrid FRPs on structural behavior of retrofitted RC beams and to investigate if different sequences of CFRP and GFRP sheets of the hybrid FRPs have influences on improvement of strengthening RC beams. The beams are loaded with different magnitudes prior to retrofitting in order to investigate the effect of initial loading on the flexural behavior of the retrofitted beam. The main test variables are sequences of attaching hybrid FRP layers and magnitudes of preloads. Under loaded condition, beams are retrofitted with two or three layers of hybrid FRPs, then the load increases until the beams reach failure. Test results conclude that strengthening effects of hybrid FRPs on ductility and stiffness of RC beams depend on orders of FRP layers.

2.1.2 Continuous Beam

Although several research studies have been conducted on the strengthening of simply supported reinforced concrete beams using external plates, there is very less reported work on the behaviour of strengthened continuous beams. Moreover, most design guidelines have been developed for simply supported beams with external FRP laminates. A critical literature review revealed that a minimum amount of research work had been done for addressing the possibility of strengthening the negative moment region of continuous beam using FRP materials. Grace et al., (1999) tested five continuous beams. Four different strengthening systems were examined. The first beam was strengthened only for flexure, while the second beam was strengthened for both flexure and shear. The third beam was strengthened with glass fibre reinforced polymer (GFRP) sheets, and the fourth beam was strengthened by using CFRP plates. The fifth beam was fabricated as control beam. All the beams were loaded and unloaded for at least one loading cycle before failure. The use of FRP laminates to strengthen continuous beams was effective for reducing deflections and for increasing their load carrying capacity. It was also concluded that the beams strengthened with FRP laminates exhibit smaller and better distributed cracks.

Grace et al., (2001) investigated the experimental performance of CFRP strips used for flexural strengthening in the negative moment region of a full-scale reinforced concrete beam. They considered two categories of beams (I and II) for flexural strengthening. Category I beams were designed to fail in shear and Category II beams were designed to fail in flexure. Five full scale concrete beams of each category were tested. It was found that Category I beams failed by diagonal cracking with local debonding at the top of the beams, meanwhile Category II beams failed by delamination at the interface of the CFRP strips and the concrete surface, both with and without concrete-cover failure by means shear/tension delamination. When the beams failed, the CFRP strips were not stressed to their maximum capacity, which led to ductile failures in all the beams. The maximum increase of load-carrying capacity due to strengthening was observed to be 29% for Category I beams, and 40% for Category II beams with respect to corresponding control beams.

On the other hand, Grace et al., (2005) performed another research work where three continuous beams were tested. One of those beam was considered as the reference beam and conventional ductile flexural failure occurred. They strengthened the other two beams along their negative and positive moment regions around the top and bottom face on both sides as a U-wrap. It was concluded that the strengthened beams with the triaxial fabric showed greater ductility than those strengthened with CFRP sheets.

In another research, El-Refaie et al., (2003) examined 11 reinforced concrete (RC) two-span beams strengthened in flexure with external bonded CFRP sheets. According to the arrangement of the internal steel reinforcement, the beams were classified into two groups. Each group included one non-strengthened reference beam. It was noted that, all strengthened beams exhibited less ductility compared with the non-strengthened control beams. An optimum number of CFRP layers were found beyond which there was no further

enhancement in the beam capacity. It was also investigated that extending the CFRP sheet length to cover the entire hogging or sagging zones did not prevent peeling failure of the CFRP sheets, which was the dominant failure mode of tested beams.

More recently, El-Refaie et al., (2003) tested five reinforced concrete continuous beams strengthened in flexure with external CFRP laminates. All beams had the same geometrical dimensions and internal steel reinforcement. The main parameters examined were the position and form of the CFRP laminates. Three of the beams were strengthened using different lay-up arrangements of CFRP reinforcement, and one was strengthened using CFRP sheets. The performance of the CFRP strengthened beams was compared with a non-strengthened reference beam. It was found that, peeling failure was the principal failure mode for all the strengthened tested beams. It was found that the longitudinal elastic shear stresses at the adhesive/concrete interface calculated at beam failure were close to the limiting value recommended in (Concrete Society Technical Report 55, 2000). They also found that, strengthened beams at both sagging and hogging zone produced the highest load capacity.

Ashour et al., (2004) tested 16 reinforced concrete (RC) continuous beams with different arrangements of internal steel bars and external CFRP laminates. All test specimens had the same geometrical dimensions and were classified into three groups according to the amount of internal steel reinforcement. Each group included one non-strengthened control beam designed to fail in flexure. Three failure modes were observed, namely laminate rupture, laminate separation and peeling failure of the concrete cover attached to the composite laminate. The ductility of all strengthened beams was reduced in comparison with their respective reference beam. Additionally, simplified methods for estimating the flexural load capacity and the interface shear stresses between the adhesive and the concrete material were presented. As in previous studies, they observed that increasing the CFRP sheet length in order to cover the entire negative or positive moment zones did not prevent peeling failure of the CFRP laminates.

Aiello et al., (2007) compared the behaviour between continuous RC beams strengthened with of CFRP sheets at negative or positive moment regions and RC beams strengthened at both negative and positive moment regions. All the beams were strengthened with one CFRP sheet layer and with the remark that the beams were not loaded at the middle of span. The control beams underwent a typical flexural and failure of the strengthened beams occurred by debonding of the CFRP sheets, together with concrete crushing. It was found out that when the strengthening was applied to both hogging and sagging regions, the ultimate load capacity of the beams was the highest and about 20% of moment redistribution could be achieved by CFRP sheets externally glued in the sagging region.

Recently, Maghsoudi et al., (2009) examined the flexural behaviour and moment redistribution of reinforced high strength concrete (RHSC) continuous beams strengthened with carbon fibre. They observed that by increasing the number of CFRP layers, the ultimate strength increases, meanwhile ductility, moment redistribution, and ultimate strain of CFRP sheet decrease. Test results also showed that by increasing the number of CFRP sheet layers, there was a change in the failure mode from tensile rupture to IC debonding. End U-straps were effective in limiting end debonding, but not intermediate span debonding.

Again, Akbarzadeh et al., (2010) conducted an experimental program to study the flexural behaviour and moment redistribution of reinforced high strength concrete (RHSC) continuous beams strengthened with CFRP and GFRP sheets. As the previous work, test results showed that by increasing the number of CFRP sheet layers, the ultimate strength increases, while ductility, moment redistribution, and ultimate strain of CFRP sheet decrease. However, by using the GFRP sheets in strengthening the continuous beams, it is possible to reduce the loss in ductility and moment redistribution but a significant increase in the ultimate strength cannot be achieved. The moment enhancement ratio of the strengthened continuous beams was significantly higher than the ultimate load enhancement ratio for the same beam. They also developed an analytical model for moment–curvature and load capacity which they used for the tested continuous beams in this current study and in other similar researches.

Finally, Majid Mohammed Ali Kadhim (2011) focused on the behavior of the high strength concrete continuous beam strengthened with carbon fibre-reinforced polymer (CFRP) sheet with different CFRP sheet lengths. Three full-scale continuous beams are analyzed under two points load, and the data of analysis are compared with the experimental data provided by other researchers. ANSYS program is used and the results obtained from analysis give good agreement with experimental data with respect to load–deflection curve, ultimate strength, and the crack patterns. The length of CFRP sheet is changed in the negative and positive regions and the results showed that the ultimate strength of the beam was reached when the value of Lsheet/Lspan reaches 1.0, and when the value decreases, the ultimate strength of beam also decreases a little (1.4%), but when it decreases less than 0.6, the ultimate strength also decreases a lot (15%).

From the above information, it is, thus, clear that there lies a vast scope of research in the field of retrofitting of RC continuous beam. Although a great deal of research has been carried out on simply supported reinforced concrete (RC) beams strengthened with Fibre Reinforced Polymer composites (FRP), a few works has been focused on continuous beams.

2.2 Objective and Scope of the Present Work

The objective of this work is to carry out the investigation of externally bonded RC continuous beams using FRP sheet. In the present work, behavior of RC continuous rectangular beams strengthened with externally bonded GFRP is experimentally studied. The beams are grouped into two series labeled S1 and S2. Each series have different longitudinal and transverse steel reinforcement ratios. All beams have the same geometrical dimensions. These beams are tested up to failure by applying two points loading to evaluate the enhancement of flexural strength due to strengthening. A finite element model has been developed to study the response of strengthened beams.

III.   Experimental Study

The experimental study consists of casting of fourteen large scale continuous (two-span) rectangular reinforced concrete beams. All the beams weak in flexure are casted and tested to failure. The beams were grouped into two series labeled S1 and S2. Each series had different longitudinal and transverse steel reinforcement ratios which are mentioned in Table 3.6 and Table 3.7 for S1 and S2 respectively. Beams geometry as well as the loading and support arrangements are illustrated in Figure 3.6. All beams had the same geometrical dimensions: 150 mm wide × 200 mm deep × 2300 mm long. One beam from each series (S1 and S2) was not strengthened and was considered as a control beam, whereas all other beams from both the series were strengthened with externally bonded GFRP sheets. Experimental data on load, deflection and failure modes of each of the beams are obtained. The change in load carrying capacity and failure mode of the beams are investigated for different types of strengthening pattern.

3.1 Casting of Specimen

For conducting experiment, the proportion of **1: 1.67: 3.33** is taken for cement, fine aggregate and course aggregate. The mixing is done by using concrete mixture. The beams are cured for 28 days. For each beam six concrete cube specimens were made at the time of casting and were kept for curing. The uniaxial compressive tests on produced concrete (150 × 150 × 150 mm concrete cube) were performed and the average concrete compressive strength (fcu) after 28 days for each beam is shown in Table 3.6 and Table 3.7.

Table 3.1 Design Mix Proportions

Description	Cement	Sand (Fine Aggregate)	Course Aggregate	Water
Mix Proportion (by weight)	1	1.67	3.33	0.55
Quantities of materials (Kg/m³)	368.42	533.98	1231.147	191.58

3.1.1 Materials for Casting
3.1.1.1   Cement
Portland Slag Cement (PSC) (Brand: Konark) is used for the experiment. It is tested for its physical properties in accordance with Indian Standard specifications. It is having a specific gravity of 2.96.
(i)   Specific gravity : 2.96
(ii) Normal Consistency : 32%
(iii)Setting Times : Initial : 105 minutes Final : 535 minutes.
(iv) Soundness : 2 mm expansion
(v)   Fineness : 1 gm retained in 90 micron sieve
3.1.1.2   Fine Aggregate
The fine aggregate passing through 4.75 mm sieve and having a specific gravity of 2.67 are used. The grading zone of fine aggregate is zone III as per Indian Standard specifications.
3.1.1.3   Coarse Aggregate
The coarse aggregates of two grades are used one retained on 10 mm size sieve and another grade contained aggregates retained on 20 mm sieve. It is having a specific gravity of 2.72.
3.1.1.4   Water
Ordinary tap water is used for concrete mixing in all the mix.
3.1.1.5   Reinforcing Steel
All the beams were grouped into two series labeled S1 and S2. Each series had different longitudinal and transverse steel reinforcement ratios which are mentioned in Table 3.6 and Table 3.7.
Series S1 beams are reinforced with two 8 mm diameter at the bottom, two 12 mm diameter bars as top

reinforcement throughout the length and two 10 mm diameter bars at top tension zone. To strengthen the beam in shear, two different diameter bars is used for stirrups, 10 mm diameter is used in the shear zone of intermediate support and 8mm diameter is used in the zone of end support. The diameter variation is given due to higher shear force in intermediate or continuous support than end support. Series S2 beams were reinforced with two high-yield Strength Deformed bars of 10 mm diameter at the bottom and two 10 mm diameter bars at top tension zone, 6 mm bars were used as hanger bars, closed stirrups of 8 mm diameter high-yield Strength Deformed bars at 100 mm centres were provided to prevent shear failure.

Three bars of each diameter rods were tested in tensile and the measured average yield strength is averaged and shown in Table 3.3. The modulus of elasticity of steel bars was 2×10^5 MPa.

Table 3.2 Tensile Strength of the bars

Diameter of the reinforcement (mm)	Tensile strength (MPa)
8	523
10	429
12	578

3.1.2 Detailing Of Reinforcement
For the same series of continuous reinforced concrete beams, same arrangement for flexure and shear reinforcement is made.
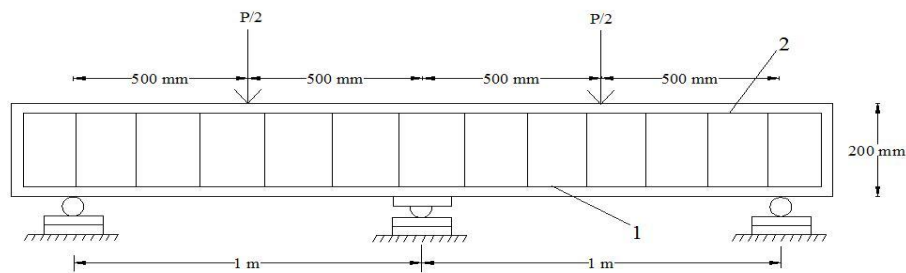
Figure 3.1 Detailing of reinforcement 1, 2 – top and bottom steel reinforcement
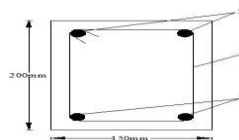
Figure 3.2 Cross section: 1 – Longitudinal rebars, 2 – close stirrups

3.1.3 Form Work

Figure 3.3 Steel Frame Used For Casting of Beam

3.1.4 Mixing Of Concrete
Mixing of concrete is done thoroughly with the help of machine mixer so that a uniform quality of concrete is obtained.

3.1.5 Compaction
Needle vibrator was used for proper Compaction and care is taken to avoid displacement of the reinforcement cage inside the form work. Then the surface of the concrete is leveled and smoothened by metal trowel and wooden float.

3.1.6 Curing Of Concrete

Curing is done to prevent the loss of water which is essential for the process of hydration and hence for hardening. Here curing is done by spraying water on the jute bags spread over the surface for a period of 28 days.

3.2 Strengthening Of Beams

At the time of bonding of fiber, the concrete surface is made rough using a coarse sand paper texture and then cleaned with an air blower to remove all dirt and debris. The fabrics are cut according to the size and after that the epoxy resin is mixed in accordance with manufacturer's instructions. The mixing is carried out in a plastic container (100 parts by weight of Araldite LY 556 to 10 parts by weight of Hardener HY 951). After the uniform mixing, the epoxy resin is applied to the concrete surface. Then the GFRP sheet is placed on top of epoxy resin coating and the resin is squeezed through the roving of the fabric with the roller. Air bubbles entrapped at the epoxy/concrete or epoxy/fabric interface are eliminated. This operation is carried out at room temperature. Concrete beams strengthened with glass fiber fabric are cured for at least 7 days at room temperature before testing.

Figure 3.4 Application of epoxy and hardener on the beam

Figure 3.5 Roller used for the removal of air bubble

3.3 Experimental Setup

The beams are tested in the loading frame of the "Structural Engineering" Laboratory of National Institute of Technology, Rourkela. The testing procedure for the all the specimen is same. The two-point loading arrangement is used for testing of beams. Two-point loading is conveniently provided by the arrangement shown in Figure 3.6.

The load is transmitted through a load cell and spherical seating on to a spreader beam. The spreader beam is installed on rollers seated on steel plates bedded on the test member with cement in order to provide a smooth leveled surface. The test member is supported on roller bearings acting on similar spreader plates. The specimen is placed over the two steel rollers bearing leaving 150 mm from the ends of the beam. The remaining 1000 mm is divided into two equal parts of 500 mm. Two dial gauges are placed just below the center of the mid span of the beam i.e. just below the load point for recording the deflection of the beams.
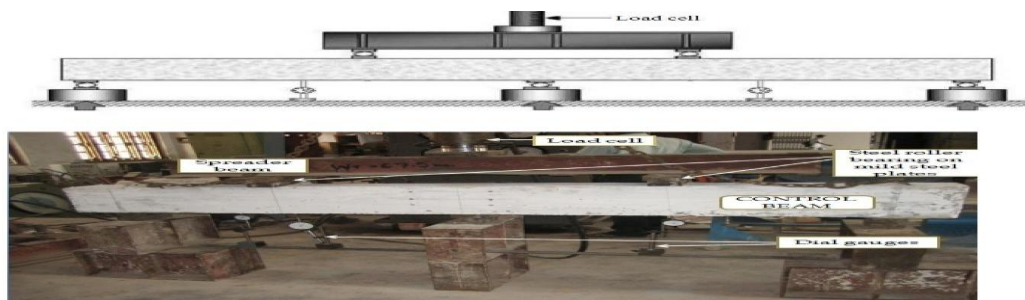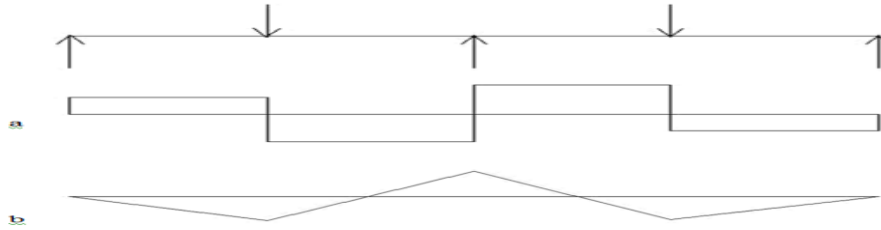
Figure 3.6 Experimental setup

Figure 3.7 Continuous beam (a) Shear Force Diagram (b)Bending Moment Diagram

3.4 Fabrication of GFRP Plate

There are two basic processes for moulding: hand lay-up and spray-up. The hand lay-up process is the oldest and simplest fabrication method. The process is most common in FRP marine construction. In hand lay-up process, liquid resin is placed along with FRP against finished surface. Chemical reaction of the resin hardens the material to a strong light weight product. The resin serves as the matrix for glass fiber as concrete acts for the steel reinforcing rods.

The following constituent materials were used for fabricating plates:
1. Glass Fiber
2. Epoxy as resin
3. Diamine as hardener as (catalyst)
4. Polyvinyl alcohol as a releasing agent

A plastic sheet was kept on the plywood platform and a thin film of polyvinyl alcohol was applied as a releasing agent by the use of spray gun. Laminating starts with the application of a gel coat (epoxy and hardener) deposited in the mould by brush, whose main purpose was to provide a smooth external surface and to protect fibers from direct exposure from the environment. Steel roller was applied to remove the air bubbles. Layers of reinforcement were applied and gel coat was applied by brush. Process of hand lay-up is the continuation of the above process before gel coat is hardened. Again a plastic sheet was applied by applying polyvinyl alcohol inside the sheet as releasing agent. Then a heavy flat metal rigid platform was kept top of the plate for compressing purpose. The plates were left for minimum 48 hours before transported and cut to exact shape for testing.

Plates of 2 layers, 4 layers, 6 layers and 8 layers were casted and six specimens from each thickness were tested.
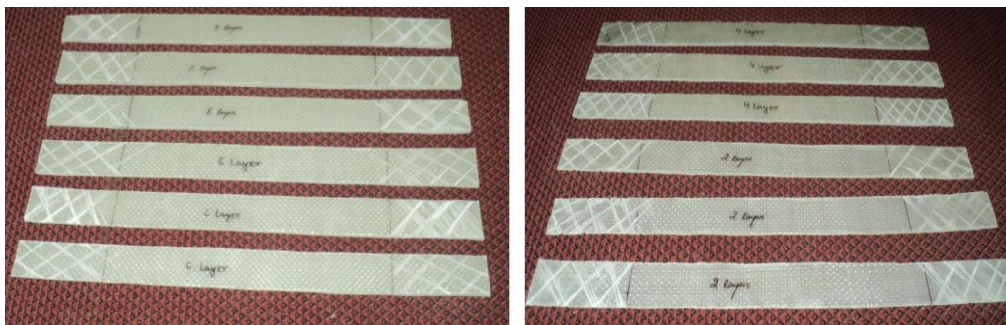
Figure 3.8 Specimens for tensile testing

Figure 3.9 Experimental set up of INSTRON 1195

Figure 3.10 Specimen failure after tensile test

Table 3.3 Size of the specimens for tensile test

No. of layers	Length (cm)	Width (cm)	Thickness (cm)
2	15	2.3	0.1
4	15	2.3	0.25
6	15	2.3	0.3
8	15	2.3	0.45

3.5 Determination of Ultimate Stress, Ultimate Laod and Young's Modulus

The ultimate stress, ultimate load and young's modulus was determined experimentally by performing unidirectional tensile test on the specimens cut in longitudinal and transverse direction. The dimensions of the specimens are shown in Table 3.4. The specimens were cut from the plates by diamond cutter or by hex saw. After cutting by hex saw, it was polished in the polishing machine. For measuring the young's modulus, the specimen is loaded in INSTRON 1195 universal tensile test machine to failure with a recommended rate of extension. Specimens were gripped in the upper jaw first and then gripped in the movable lower jaw. Gripping of the specimen should be proper to prevent slippage. Here, it is taken as 50 mm from each side. Initially, the stain is kept zero. The load as well as extension was recorded digitally with the help of the load cell and an extensometer respectively. From these data, stress versus stain graph was plotted, the initial slope of which gives the Young's modulus. The ultimate stress and the ultimate load were obtained at the failure of the specimen. The average value of each layer of the specimens is given in the Table 3.5.

Table 3.4 Result of the specimens

Thickness of the specimen	Ultimate stress (MPa)	Ultimate Load (N)	Young's modulus(MPa)
2 Layers	172.79	6200	6829.9
4 Layers	209.09	9200	7788.5
6 Layers	236.23	12900	7207.4
8 Layers	253.14	26200	7333.14

3.6 Testing Of Beams

All the fourteen beams are tested one by one. All of them are tested in the above arrangement. The gradual increase in load and the deformation in the dial gauge reading are taken throughout the test. The load at which the first visible crack is developed is recorded as cracking load. Then the load is applied till the ultimate failure of the beam. The deflections at midpoint of each span are taken for all beams with and without GFRP and are recorded with respect to increase of load. The data furnished in this chapter have been interpreted and discussed in the next chapter to obtain a conclusion.

Table 3.5 Details of the Test Specimens for Series S1

Designation of Beams	fcu (MPa)	Main Longitudinal steel		Positive moment strengthening		Negative moment strengthening	
		Top	Bottom	No. of layers	Strengthened length(m)	No. of layers	Strengthened length(m)
CB1	22.67	2-12 2-10*	2-8	-	-	-	-
SB1	23.3	2-12 2-10*	2-8	2	0.88m	6	0.88m
SB2	25.82	2-12 2-10*	2-8	1			
SB3	23.85	2-12 2-10*	2-8	2			
SB4	24.46	2-12 2-10*	2-8	3			
SB5	24.68	2-12 2-10*	2-8	4			
SB6	22.86	2-12 2-10*	2-8	4			
SB7	25.3	2-12 2-10*	2-8	2		4	
SB8	25.13	2-12 2-10*	2-8	3		6	
SB9	23.9	2-12 2-10*	2-8	2			

*provided at top tension zone

Table 3.6 Details of the Test Specimens for Series S2

Designation of Beams	fcu (MPa)	Main Longitudinal steel		Positive moment strengthening		Negative moment strengthening	
		Top	Bottom	No. of layers	Strengthened length(m)	No. of layers	Strengthened length(m)
CB2	25.34	2-6, 2-10*	2-10	0	-	0	-
TB1	24.5	2-6, 2-10*	2-10	2	0.88m	6	0.88m
TB2	23.51	2-6, 2-10*	2-10	2			
TB3	25.61	2-6, 2-10*	2-10	4			

*provided at top tension zone

3.6.1 BEAM-1
CONTROL BEAM (CB1)

The control beam, CB1, failed in the RC conventional flexural mode due to yielding of internal tensile steel reinforcement. The wide flexural cracks were occurred at mid-span and central support. These cracks were well extended to the compressive regions.

Figure 3.11 Experimental Setup of the CB1

Figure 3.12 Flexural failure of CB1

3.6.2 BEAM-2
CONTROL BEAM (CB2)
The control beam, CB2 also failed in flexural failure as shown in Figure 3.13.

Figure 3.13 Control Beam, CB2 after failure

3.6.3 BEAM-3
STRENGHENED BEAM 1 (SB1)
The beam was strengthened by applying two layers of FRP below the beam (width= 150 mm) from support to support and six layers of FRP above the central support (width= 150 mm) between two load points as shown in Figure 3.14. The strengthened beam SB1, showed crack at a load of 110 KN and failed by debonding failure in which the FRP sheet was separated without concrete cover and the ultimate failure occurred at 320KN as shown in Figure 3.15. The rupture of FRP sheet was sudden and accompanied by a loud noise indicating a rapid release of energy and a total loss of load capacity.

Figure 3.14 Experimental Setup of the Beam

Figure 3.15 Debonding failure of FRP

Figure 3.16 Magnified view of the failure of the beam

3.6.4 BEAM-4
STRENGHENED BEAM 2 (SB2)

Single layer of U-wrap was applied on the beam to prevent flexural failure. Tensile rupture of FRP occurred at the mid section of both left and right span at lower loads and as the load increased, the beam failed in debonding with concrete cover as shown in Figure 3.17 and shear crack was developed below the FRP layer as shown in Figure 3.18.
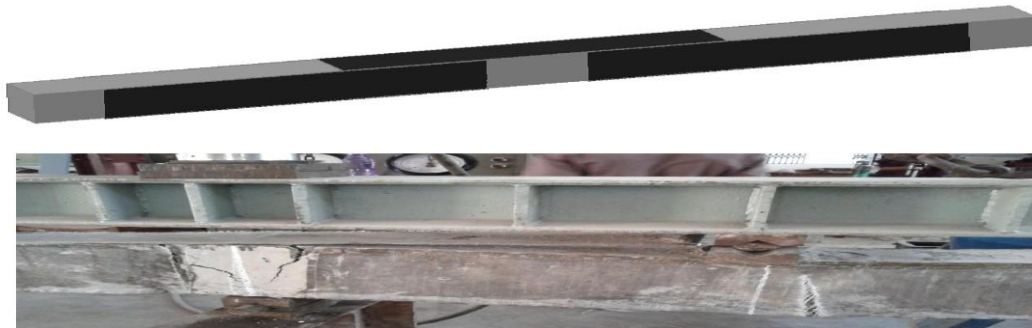
Figure 3.17 Tensile rupture of FRP at mid section of right span at lower value of load

Figure 3.18 Ultimate failure of beam by debonding of FRP with concrete cover

3.6.5 BEAM-5
STRENGHENED BEAM 3 (SB3)

U- Jacketed double Layered GFRP was applied to enhance the load capacity as shown in the Figure3.19. By strengthening the RC beam using GFRP sheet, the cracking of the beam can be delayed and flexural capacity can be increased. The strengthened beam failed in debonding of FRP sheet (Figure 3.20).

Figure 3.19 U-jacketed GFRP wrapped on the Beam SB3

Figure 3.20 Debonding failure of FRP

3.6.6 BEAM-6
STRENGHENED BEAM 5 (SB4)

To prevent debonding, one layer of complete U-wrap was provided above the FRP of two layers which was applied at the soffit of the beam (width =150 mm) and one layer of U-strip of width 10 cm was applied over 6 layers FRP above the central support. Complete U-wrap took extra load and prevented the debonding, the failure mode was tensile rupture and as the U-strip could not prevent debonding of upper layer of FRP as it got ruptured at higher load value.

Figure 3.21 Strengthening pattern of beam SB4

Figure 3.22 Crack pattern after initial loading

Figure 3.23 Failure of the beam by tensile rupture

3.6.7 BEAM-7
STRENGHENED BEAM 5 (SB5)

Same arrangement of FRP was made as SB4 and to enhance the capacity of beam SB4, two layers of complete U-wrap was provided in place of one layer and layers of U-strip of width 10 cm was applied instead of one layer.

Figure 3.24 Cracking pattern at lower load value

Figure 3.25 Rupture of GFRP sheet at mid section of the right span

3.6.8 BEAM-8
STRENGHENED BEAM 6 (SB6)

Above the U- Jacketed double Layered GFRP, more two layers of FRP but half of the width of the first two layers, was applied at the flexural zone to prevent the flexural failure. In this case, instead of tensile rupture, debonding failure occurred as shown in Figure 3.27.

Figure 3.26 Debonding of FRP and cracking pattern above central support of the beam

Figure 3.27 Debonding failure of Strengthened beam SB6

3.6.9 BEAM-9
STRENGHENED BEAM 7 (SB7)
The depth of the neutral axis was found out and the GFRP was provided up to the Neutral axis from the tension face. Here, shear crack was found and debonding occurred as shown in Figure 3.29.
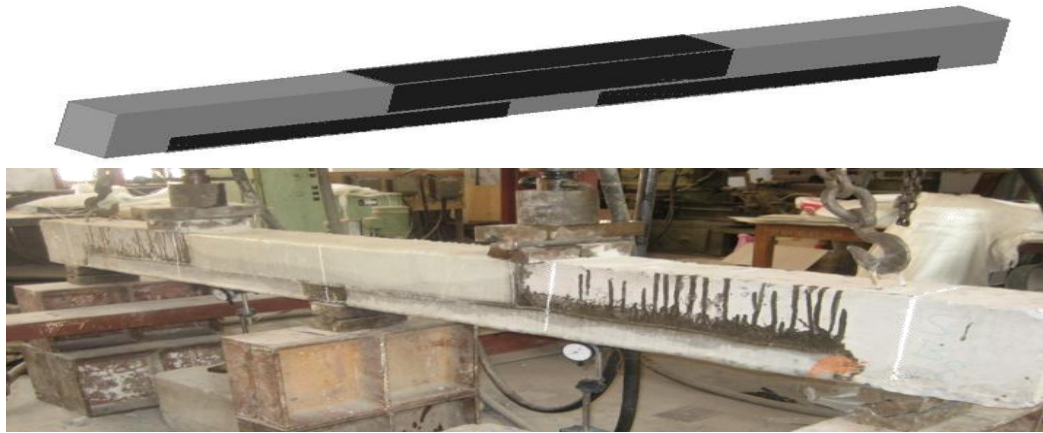
Figure 3.28 Strengthening pattern of SB7

Figure 3.29 Shear crack in the left span

Figure 3.30 Magnified view of shear crack and debonding of GFRP

3.6.10 BEAM-10
STRENGHENED BEAM 8 (SB8)
The no. of FRP layers was increased here as compared to SB7 to examine the changes in load capacity or the failure pattern. The failure mode of the beam was debonding as shown in Figure 3.32.

Figure 3.31 Strengthening pattern of SB8

Figure 3.32 Failure of SB8 by debonding of GFRP

3.6.11 BEAM-11
STRENGHENED BEAM 9 (SB9)

To prevent debonding of FRP, steel bolt system was introduced. The holes in the beam were made while casting of the beam and after applying FRP sheet to the beam the steel bolts were inserted into the hole and were tightened after placing the steel plate after the FRP. Anchoring plate, because of high compressive stress got buckled as shown in Figure 3.34.
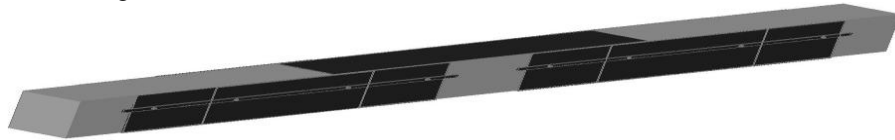
Figure 3.33 Strengthening and anchoring pattern of SB9

Figure 3.34 Failure pattern of SB9

Figure 3.35 Magnified view of Debonding

3.6.12 BEAM-12
TB1

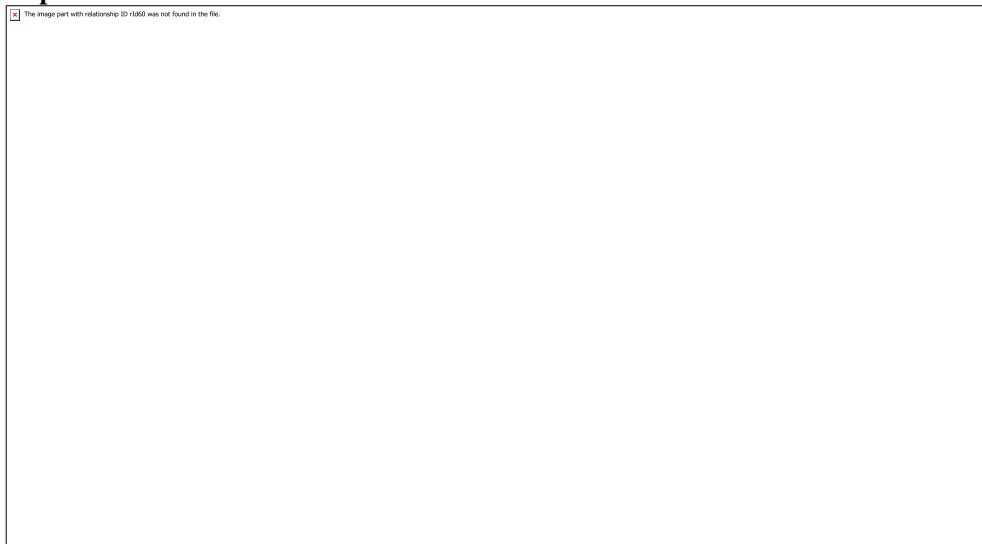The strengthened beam showed crack at a load of 110 KN and failed by debonding failure in which the FRP sheet was separated without concrete cover at 224 KN which is shown in Figure 3.37. The rupture of FRP sheet was sudden and accompanied by a loud noise indicating a rapid release of energy and a total loss of load capacity. By strengthening the RC beam using GFRP sheet, the cracking of the beam can be delayed and flexural capacity can be increased.

Figure 3.36 Top FRP of Beam TB1 before Testing

Figure 3.37 FRP sheet separations without concrete

3.6.13 BEAM-13
TB2

Full double layered U-wrap was applied and six layers of FRP above the central support. The ultimate failure load was 298 KN.
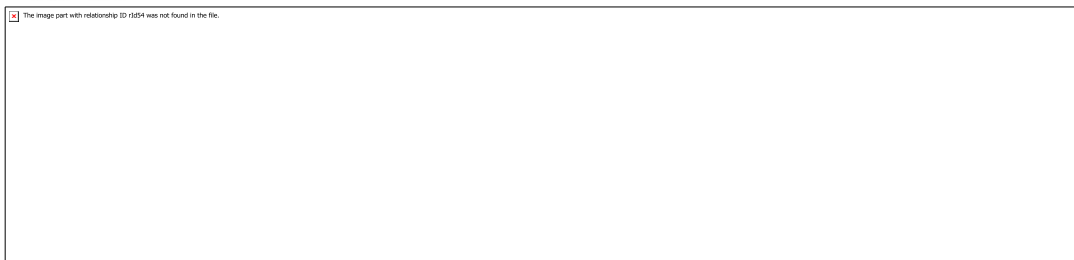
Figure 3.38 Experimental set up and strengthening pattern of TB2

Figure 3.39 Failure of the beam by tensile rupture

3.6.14 BEAM-14
TB3
Above the U- Jacketed double Layered GFRP, more two layers of FRP but half of the width of the first two layers, was applied at the flexural crack zone to prevent the flexural failure. In this case, instead of tensile rupture, debonding failure occurred as shown in Figure 3.41 and the failure load was 326 KN.

Figure 3.40 Strengthened beam TB3

Figure 3.41 Failure of beam TB3

Figure 3.42 Shear crack in the left span

Figure 3.43 Failure mode of TB3

IV. Test Results And Discussions

The beams were loaded with a concentrated load at the middle of each span and the obtained experimental results are presented and discussed subsequently in terms of the observed mode of failure and load-deflection curve. The crack patterns and the mode of failure of each beam are also described in this chapter. All the beams are tested for their ultimate strengths and it is observed that the control beam had less load carrying capacity than the strengthened beam. Two sets of beams i.e. S1 and S2 were examined and one beam from each series was tested as un-strengthened control beam and rest beams were strengthened with various patterns of FRP sheets. The different failure modes of the beams were observed for both the series S1

and S2 as shown in Table 4.1 and Table 4.2.

4.1 Experimental Results
4.1.1 Failure Modes
4.1.1.1 Control Beam
  The control beam CB1 and CB2 failed completely in flexure. The failure started first at the tension zone and then propagated towards the compression zone and finally failed in flexure.

4.1.1.2 Strengthened Beam
  Generally, the rupture of FRP sheet was sudden and accompanied by a loud noise indicating a rapid release of energy and a total loss of load capacity. For all the strengthened beams, the failure modes for Series S1 and S2 are described in Table 4.1 and Table 4.2.

The following failure modes were examined for all the tested beams:
- Flexural failure
- Debonding failure (with or without concrete cover)
- Tensile rupture

  Rupture of the FRP laminate is assumed to occur if the strain in the FRP reaches its design rupture strain before the concrete reaches its maximum usable strain. GFRP debonding can occur if the force in the FRP cannot be sustained by the substrate. In order to prevent debonding of the GFRP laminate, a limitation should be placed on the strain level developed in the laminate.

Table 4.1 Experimental Results of the Tested Beams for Series S1

The image part with relationship ID rId60 was not found in the file.

Table 4.2 Experimental Results of the Tested Beams for Series S2

Designation of Beams	Failure Mode	P_u(KN)	$\lambda = \dfrac{P_u(\text{strengthened beam})}{P_u(\text{Control beam})}$
CB2	Flexural failure	200	1
TB1	Debonding failure	224	1.12
TB2	Tensile rupture	298	1.49
TB3	Debonding of FRP	326	1.68

4.1.2 Load Deflection and Load Carrying Capacity
  The GFRP strengthened beams and the control beams are tested to find out their ultimate load carrying capacity. The deflection of each beam under the load point i.e. at the midpoint of each span position is analyzed. Mid-span deflections of each strengthened beam are compared with the control beam. It is noted that the behavior of the flexure deficient beams when bonded with GFRP sheets are better than the control beams. The mid-span deflections of the beams are lower when bonded externally with GFRP sheets. The stiffness of the

strengthened beams was higher than that of the control beams. Increasing the numbers of GFRP layers generally reduced the mid span deflection and increased the beam stiffness for the same value of applied load. The use of GFRP sheet had effect in delaying the growth of crack formation.

The ultimate failure load for all the tested beams are summarized in Table 4.1 and Table 4.2. The ultimate load enhancement ratio (λ), which is the ratio of the ultimate load of the externally strengthened beam to the control beam, is presented in Table 4.1 and Table 4.2. From the two tables it is found that, addition of GFRP layers increased the ultimate load capacity and by introducing the anchoring system, the enhancement of load capacity can be done.

4.1.2.1 Strengthened Beam of S1 Series
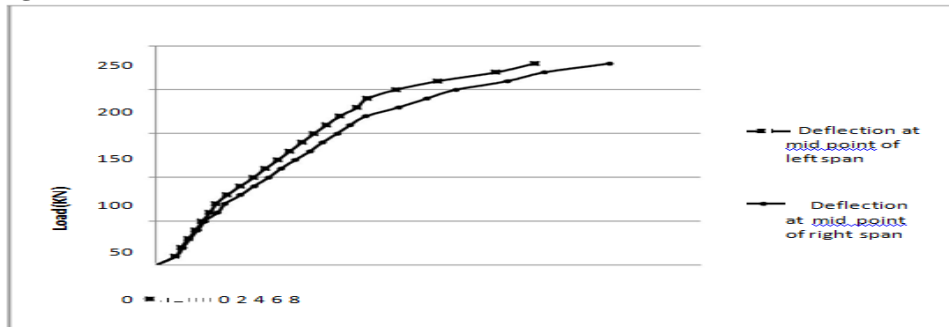
Figure 4.1 Load versus Deflection Curve for CB1

Beam 1 was taken as the control beam (CB1) which is weak in flexure and no strengthening was done to this beam. Two point static loading was applied on the beam and at the each increment of the load, deflection at midpoint of each span were taken with the help of dial gauges. Using this load and deflection data, load vs. deflection curve was plotted. At the load of 70 KN initial hairline cracks appeared. Later with the increase in loading values the crack propagated further. The Beam CB1 failed completely in flexure at the load of 260 KN.
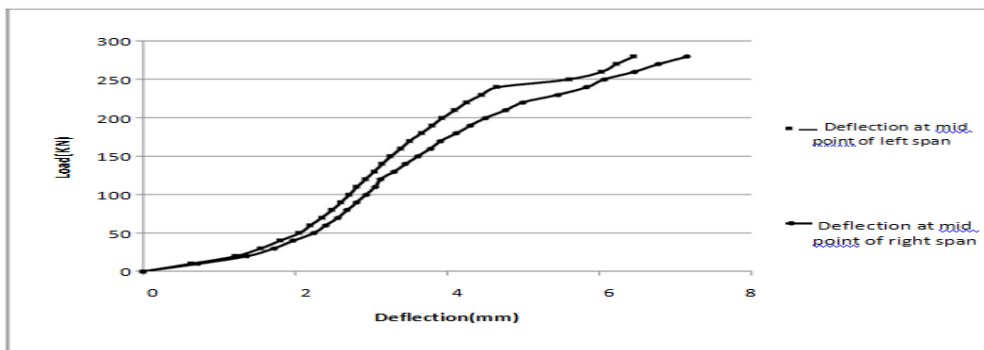
Figure 4.2 Load versus Deflection Curve for SB1

Beam-2, SB1 is strengthened by applying GFRP at the soffit from support to support and at the top between two load points. At the midpoint of each span, deflection values were taken and load versus deflection curve was plotted. The deflection values are less than that of the control beam for the same load value. At the load of 110 KN initial hairline cracks appeared. Later with the increase in loading values the crack propagated further. At lower load, debonding of FRP without concrete cover occurred and SB1 finally failed in concrete crushing with an ultimate load of 320 KN.
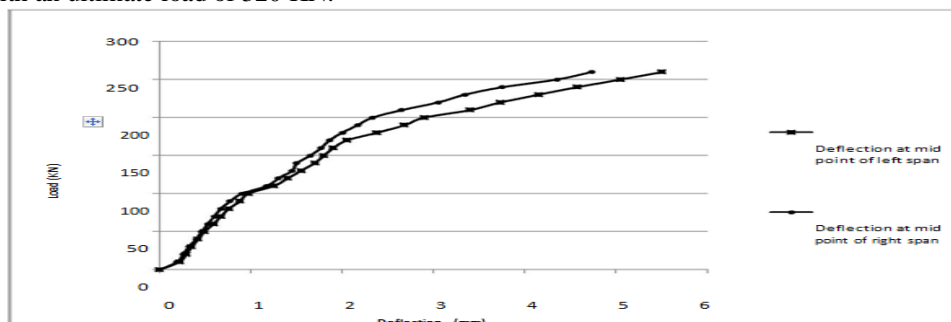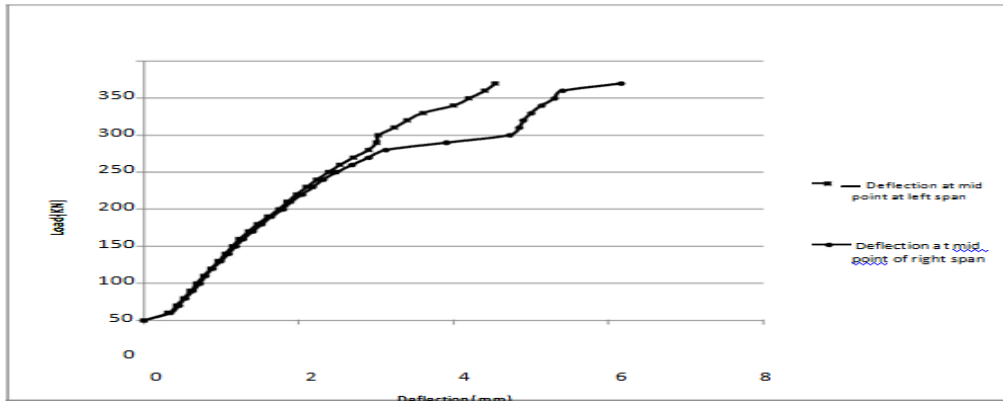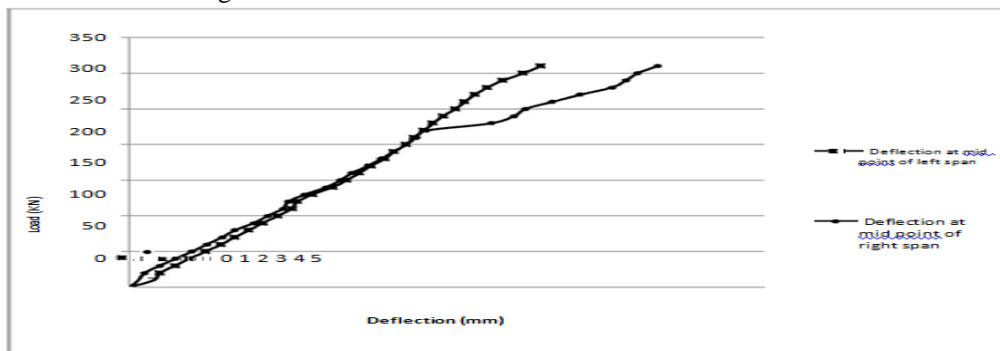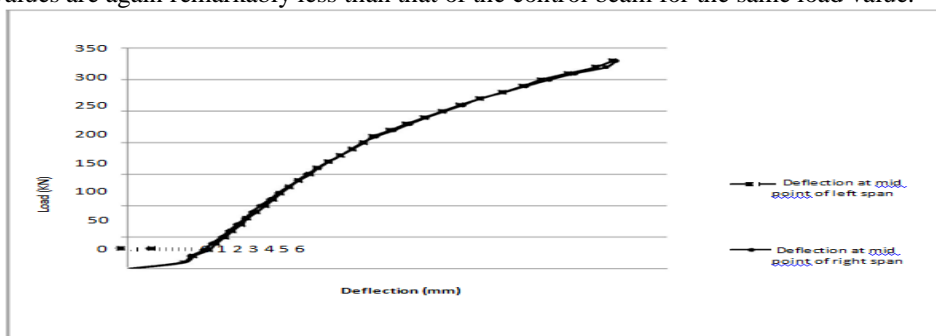

Figure 4.3 Load versus Deflection Curve for SB2

Beam-3, SB2 is strengthened with U-wrap from support to support distance and at the top of the beam between the two load points. The deflection values are less than that of the control beam for the same load value. No initial hairline cracks were visible due to the covering of GFRP. Later with the increase in loading values the crack propagated further under the GFRP. Tensile rupture took place at lower load and as the load increased, debonding of the FRP occurred with concrete cover and finally the beam failed in shear and the failure load was 325 KN.

Figure 4.4 Load versus Deflection Curve for SB3

Beam-4, SB3 is strengthened with U-wrap from support to support distance, but the layers were increased and at the top of the beam between the two load points. The beam failed in debonding of FRP without concrete cover. The deflection values are remarkably less than that of the control beam and beam SB1 for the same load value. The cracking load was 120 KN and the failure load was 334 KN.

Figure 4.5 Load versus Deflection Curve for SB4

Beam-5, SB4 is strengthened providing FRP at the soffit of the beam from support to support distance and U-wrap above it, and at the top of the beam between the two load points and U-strip above it. Tensile rupture of FRP without concrete cover occurred and later with the increase in loading values the crack propagated further under the GFRP and beam failed in flexure. The failure load of SB4 was 370 KN. The deflection values are again remarkably less than that of the control beam for the same load value.

Figure 4.6 Load versus Deflection Curve for SB5

Beam-6, SB5 is strengthened providing FRP at the soffit of the beam from support to support distance and U-wrap above it, and at the top of the beam between the two load points and U-strip above it. Here the

numbers of FRP layers of U-wrap and U-strip were increased. Tensile rupture of FRP without concrete cover occurred at lower load value and later with the increase in loading values the crack propagated further under the GFRP and beam failed in flexure. The deflection values are less than that of the control beam for the same load value. The failure load of SB5 was 380 KN. The ultimate load of this beam was higher than the beam SB4, which was having same pattern of FRP wrapping.
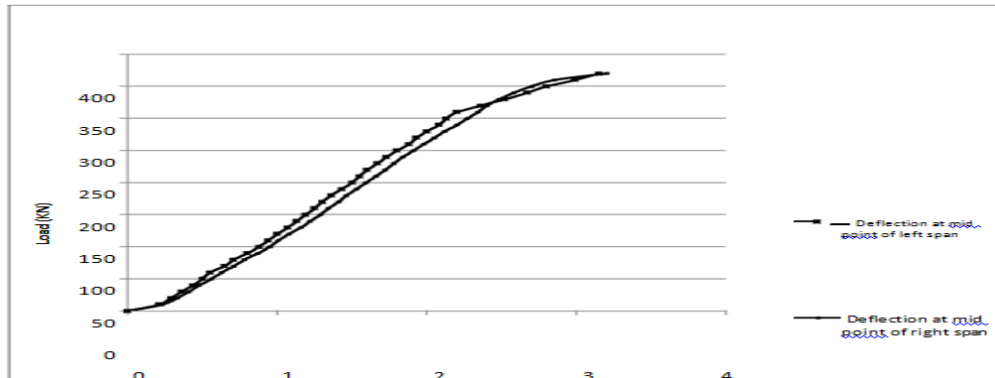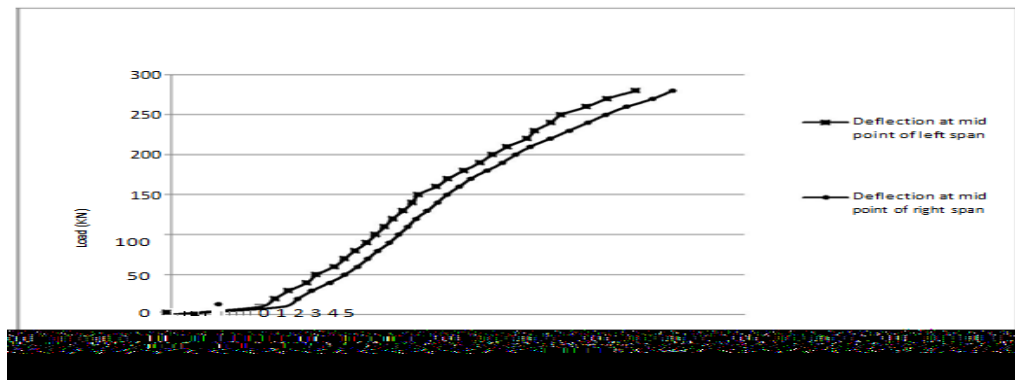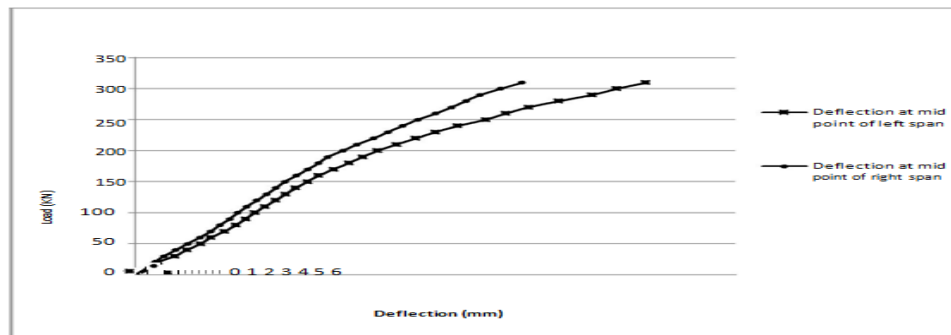

Figure 4.7 Load versus Deflection Curve for SB6

Beam-7, SB6 is strengthened providing U-wrap FRP from support to support distance and U-wrap FRP of half of the width above it, and at the top of the beam between the two load points. Debonding of FRP without concrete cover occurred first and later with the increase in loading values the crack propagated further under the GFRP and beam failed in flexure. The deflection values are quite less than that of the control beam for the same load value. The failure load of SB6 was 415 KN.

Figure 4.8 Load versus Deflection Curve for SB7

Beam-8, SB7 is strengthened providing U-wrap FRP from support to support distance up to Neutral axis and U-wrap FRP at the top of the beam between the two load points up to Neutral axis. Debonding of FRP without concrete cover occurred, with the increase in loading values the shear crack developed and propagated and beam failed in shear. The deflection values are quite less than that of the control beam for the same load value. The failure load of SB7 was 332 KN.

Figure 4.9 Load versus Deflection Curve for SB8

Beam-9, SB8 is strengthened providing U-wrap FRP from support to support distance up to Neutral axis and U-wrap FRP at the top of the beam between the two load points up to Neutral axis. Here the layers of the U-wrap were increased. Beam failed in debonding of FRP without concrete cover. Here also, the deflection

values are quite less than that of the control beam for the same load value. The failure load of SB8 was 345 KN.
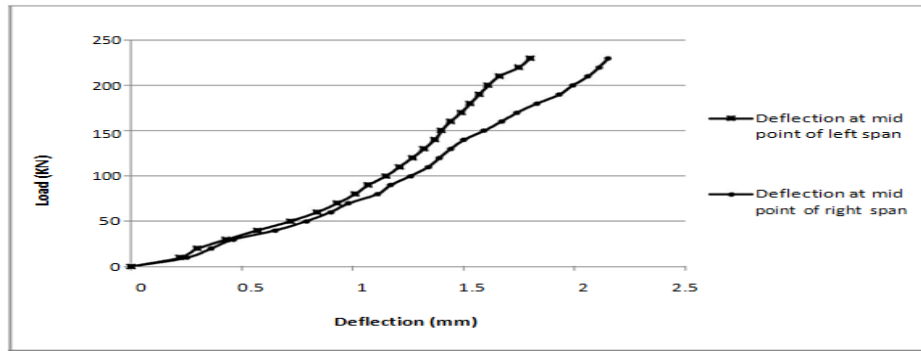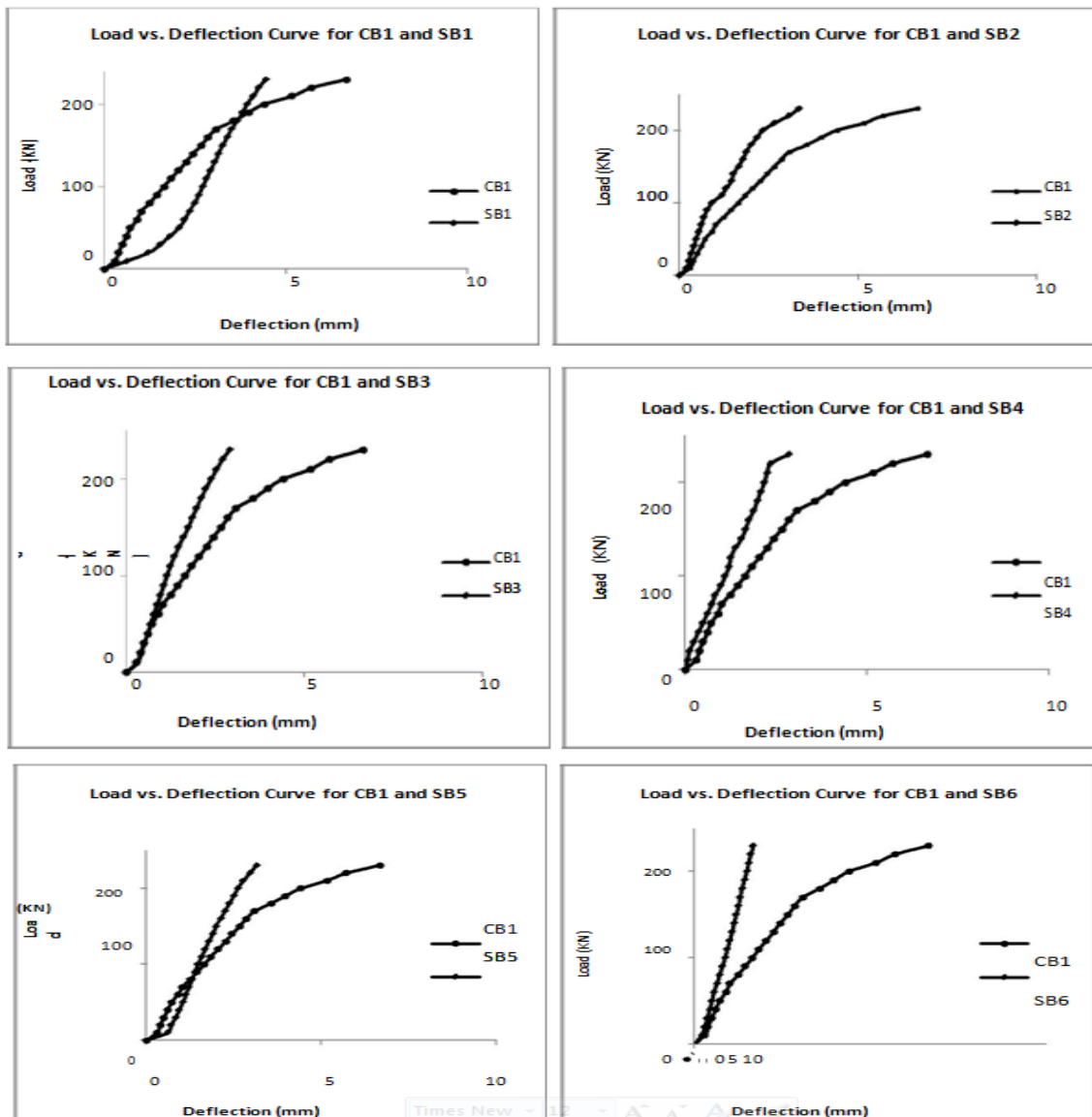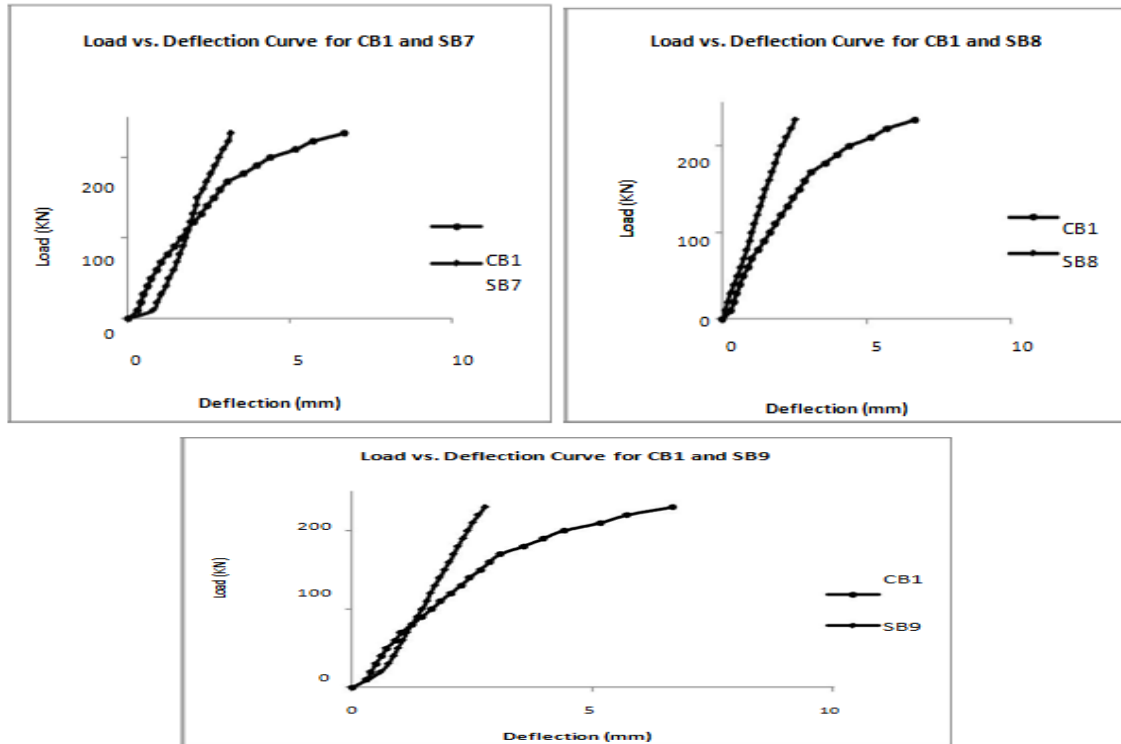

Figure 4.10 Load versus Deflection Curve for SB9

Beam-10, SB9 is strengthened as beam SB6, i.e. U-wrap FRP from support to support distance and U-wrap FRP of half of the width above it, and at the top of the beam between the two load points. Here, to prevent debonding failure anchoring system was introduced. It took more load than the corresponding beam SB6 and up to some load values it prevented the debonding failure. It prevented the debonding failure up to some extent and finally failed in flexure. The deflection values are quite less than that of the control beam for the same load value. The failure load of SB9 was 421 KN.

Figure 4.11 Load versus Deflection Curve for Set S1 strengthened beams with CB1

In Figure 4.11, the midpoint deflection values of all the strengthened beams were compared with the control beam CB1 separately and it was found that, by strengthening the beams with GFRP, the stiffness increased and the deflection value reduced up to some extent.
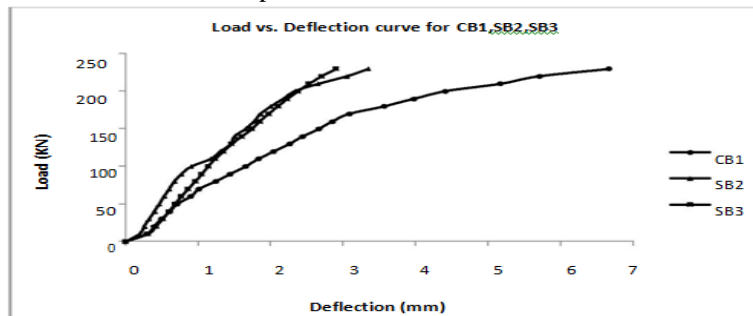
Figure 4.12 Load versus Deflection Curve for CB1, SB2, SB3

In SB2 one layer and in SB3 two layers of U-wrap were provided to strengthen the beams. The midpoint deflections were compared with the control beam and shown in Figure 4.12 from where it can be concluded that the deflection value is decreasing by strengthening the beams and by increasing the layers of GFRP, the stiffness of beam increases slightly.
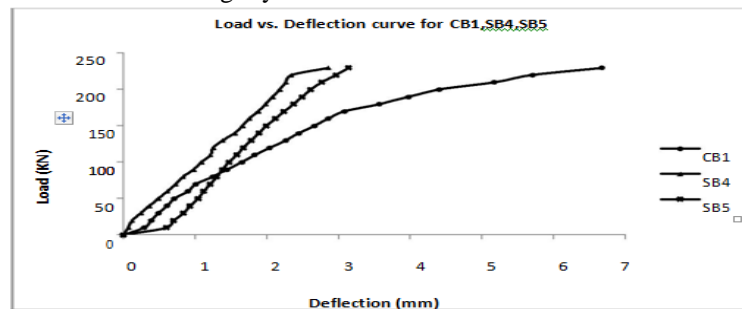
Figure 4.13 Load versus Deflection Curve for CB1, SB4, SB5

In SB4, one layer of U-wrap and U-strip and in SB5, two layers of U-wrap and two layers U-strip was

provided to strengthen the beams. The midpoint deflection was compared with the control beam and shown in Figure 4.13.
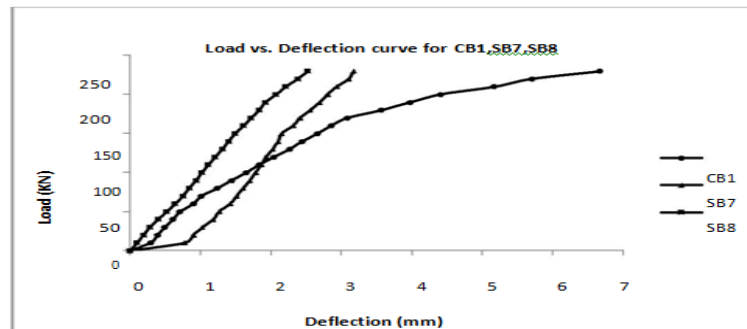

Figure 4.14 Load versus Deflection Curve for CB1, SB7, SB8

In SB7, two and four layers of U-wrap GFRP were provided below and above the Neutral axis respectively and in case of SB8 the GFRP layers were increased to three and six respectively. The midpoint deflections of SB1 and SB8 were compared to CB1 and from the plotted graphs and it is concluded that, by increasing the GFRP layers the stiffness of the beam can be increased.
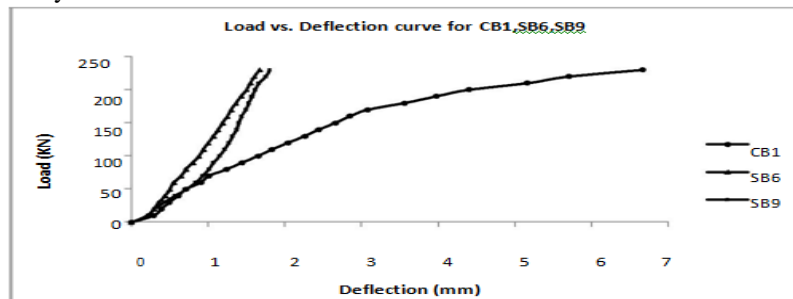
Figure 4.15 Load versus Deflection Curve for CB1, SB6, SB9

In SB9, Steel bolts were used to prevent the debonding failure of FRP. Here, the load capacity of SB9 was higher than SB6, the deflection values were less than CB1 as shown in Figure 4.15.
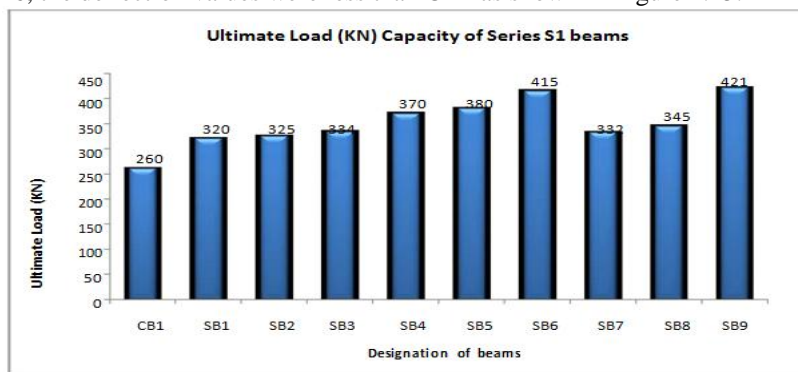

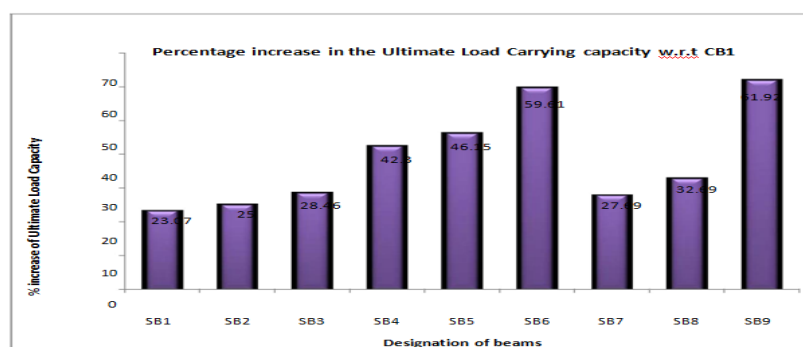Figure 4.16 Ultimate Load Capacity of Series S1 beams

Figure 4.17 Percentage increase in the Ultimate Load Carrying capacity of strengthened beams of S1 w.r.t CB1

From Figure 4.16, it is concluded that the load capacity of SB9 beam is highest and SB6 beam has second highest load capacity among all the strengthened beams of Series S1. The percentage increase of load capacity of all the beams are calculated and are drawn in Figure 4.17 from which it can be concluded that, by application of GFRP to the beams the load capacity can be enhanced. Strengthened beam SB6 and SB9 gives the maximum percentage increase of load capacity.

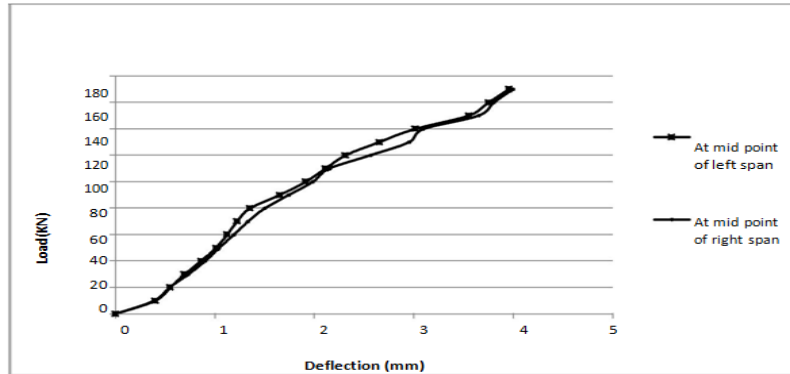**4.1.2.2 Strengthened Beam of S2 Series**

Figure 4.18 Load versus Deflection Curve for CB2

Beam 11, Control Beam for set S2, CB2, to which no external strengthening was provided, two point static loading was applied and at the each increment of the load, deflections at midpoint of each span were taken with the help of dial gauges. Using this load and deflection data, load vs. deflection curve was plotted. At the load of 110 KN initial hairline cracks appeared and the beam failed in flexure with an ultimate load value of 200 KN.
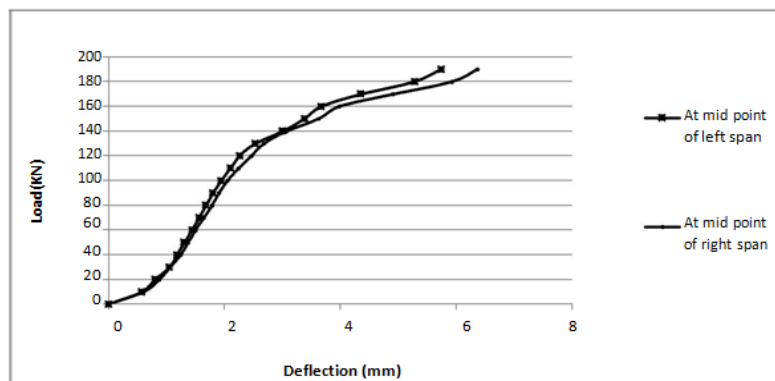
Figure 4.19 Load versus Deflection Curve for TB1

Beam-12, TB1 is strengthened at the soffit from support to support and at the top between two load points. At the midpoint of each span, deflection values were taken and load versus deflection curve was plotted. The deflection values are less than that of the control beam for the same load value. At lower load value, debonding of FRP without concrete cover occurred and TB1 finally failed in concrete crushing. At the load of 120 KN initial hairline cracks appeared. Later with the increase in loading values the cracks propagated further and the beam failed with an ultimate load of 224 KN.
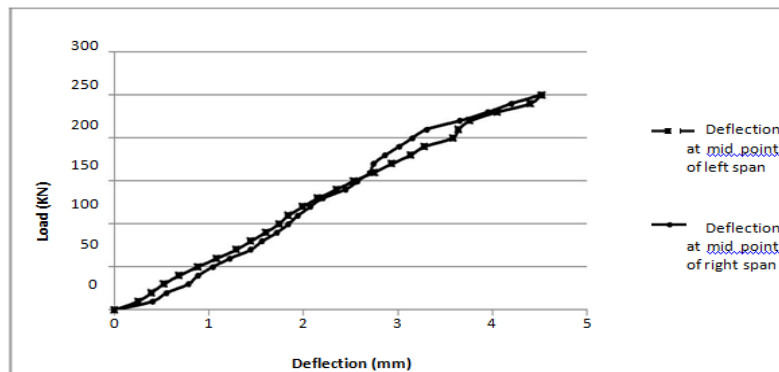
Figure 4.20 Load versus Deflection Curve for TB2

Beam-13, TB2 is strengthened with U-wrap from support to support distance and at the top of the beam between the two load points but the layers of U-wrap was increased here. The deflection values are less than that of the control beam for the same load value. The beam failed in tensile rupture followed by flexural failure. The cracking load was 210 KN and the failure load was 298 KN.
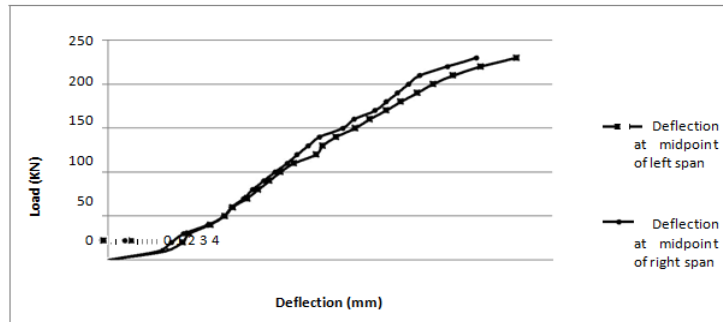
Figure 4.21 Load versus Deflection Curve for TB3

Beam-14, TB3 failed in debonding of FRP without concrete cover followed by shear crack. The deflection values are remarkably less than that of the control beam, CB2 and strengthened beam TB1 for the same load value. The failure load was 326 KN.
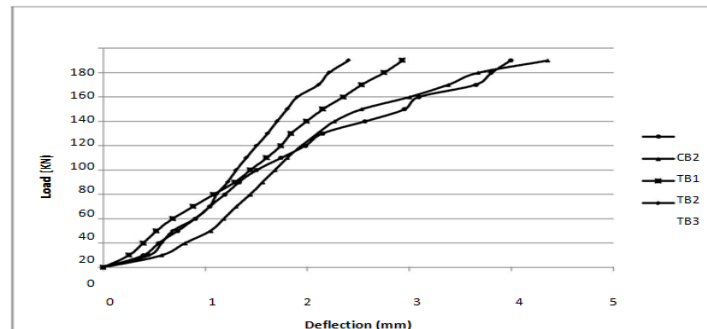
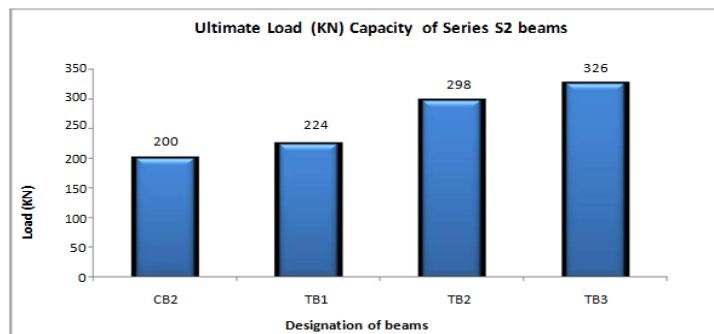Figure 4.22 Load vs. Deflection Curve for all the Beams of S2

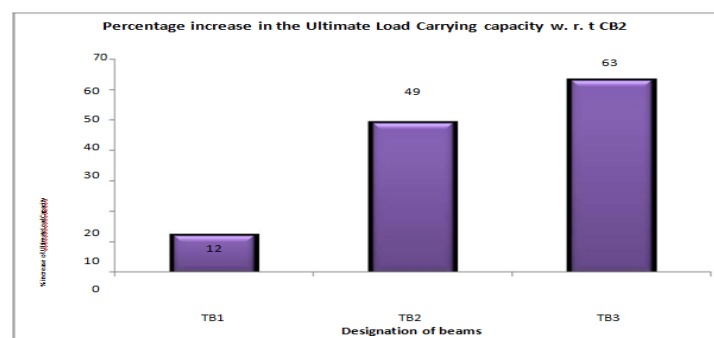Figure 4.23 Ultimate Load (KN) Capacity of Series S2 beams

Figure 4.24 Percentage increase in the Ultimate Load Carrying capacity of strengthened beams of S2 w.r.t CB2

The load capacity and the percentage increase of all the strengthened beams of series S2 are discussed here and from Figure 4.23 and Figure 4.24, it is found that beam TB3 has the maximum load capacity and maximum percentage increase of load carrying capacity respectively.

V. Finite Element Analysis

Finite element method (FEM) is a numerical method for solving a differential or integral equation. It has been applied to a number of physical problems, where the governing differential equations are available. The method essentially consists of assuming the piecewise continuous function for the solution and obtaining the parameters of the functions in a manner that reduces the error in the solution.

5.1 Formulation

The governing equation for beam is given in Equation 5.1.

$$M = \frac{d^2 y}{d x^2} EI \tag{5.1}$$

The displacement field v(x) assumed for the beam element should be such that it takes on the values of deflection and the slope at either end as given by the nodal values $v_i, \theta_i, v_j, \theta_j$.

The v(x) can be given by,

$$v(x) = c_0 + c_1 x + c_2 x^2 + c_3 x^3 \tag{5.2}$$

In solving the differential equations through integration, there will be constants of integration that must be evaluated by using the boundary and continuity conditions. The variables whose values are to be determined are approximated by piecewise continuous polynomials. The coefficients of these polynomials are obtained by minimizing the total potential energy of the system. In FEM, usually, these coefficients are expressed in terms of unknown values of primary variables. Thus, if an element has got n nodes, the displacement field u can be approximated as,

$$u = \sum_{i=1}^{n} N_i u_i \tag{5.3}$$

where u_i are the nodal displacements in x-direction and N_i are the shape functions, which are functions of coordinates. Shape functions or interpolation functions N_i are used in the finite element analysis to interpolate the nodal displacements of any element to any point within each element. The beam element has modulus of elasticity E, moment of inertia I, and length L. Each beam element has two nodes and is assumed to be horizontal as shown in Figure 5.1. The element stiffness matrix is given by the following matrix, assuming axial deformation is neglected.

$$K = \frac{EI}{L^3} \begin{bmatrix} 12 & 6L & -12 & 6L \\ 6L & 4L^2 & -6L & 2L^2 \\ -12 & -6L & 12 & -6L \\ 6L & 2L^2 & -6L & 4L^2 \end{bmatrix} \tag{5.4}$$

It is clear that the beam element has four degrees of freedom: two at each node (a transverse displacement and a rotation). The sign convention used is that the displacement is positive if it points upwards and the rotation is positive if it is counter clockwise. Consequently for a structure with n nodes, the global stiffness matrix K will be of size $2n \times 2n$ (since we have two degrees of freedom at each node). Once the global stiffness matrix K is obtained we have the following structure equation

$$[K]\{U\}=\{F\} \tag{5.5}$$

where U is the global nodal displacement vector and F is the global nodal force vector.

First the boundary conditions are applied manually to the vectors U and F. Then the matrix (5.5) is solved by partitioning and Gaussian elimination. Finally once the unknown displacements and reactions are found, the nodal force vector is obtained for each element as follows:

$\{f\} = [k] \{u\}$ (5.6)

where $\{f\}$ is the 4×1 nodal force vector in the element and u is the 4×1 element displacement vector. The first and second elements in each vector $\{u\}$ are the transverse displacement and rotation, respectively, at the first node, while the third and fourth elements in each vector $\{u\}$ are the transverse displacement and rotation, respectively, at the second node.

5.2 Validation of Experimental Value
In the experimental work, the tested beams consist of two spans of each 1000 mm as shown in Figure 5.1 is discritized as shown in Figure 5.2.
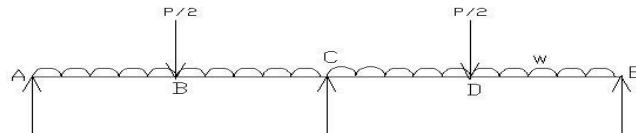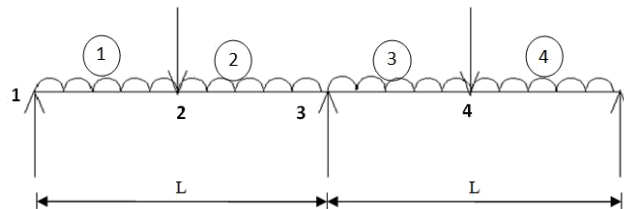

Figure 5.1 Continuous beam

Figure 5.2 Finite element model

Figure 5.3 Beam element forces

The following sign convention is considered for the deflection calculation.
(a) x is +ve towards right
(b) y is +ve upwards
(c) Anticlockwise slopes are +ve
(d) Sagging BM are +ve

Four element mesh is taken as shown in Figure 5.2. Subdividing the span AC into two elements with a node at the load point has the advantage that, the nodal forces can be specified very easily. The meshing has also ensured that all elements are of uniform size, for easy hand calculation. Following the standard procedure, the global stiffness matrix and force vector is obtained as below,

$[K]_{10 \times 10} \{U\}_{10 \times 1} = \{F\}_{10 \times 1}$ (5.7)

Since there are five nodes and two d.o.f. per node, the global stiffness matrix is of size (10×10) and $\{F\}$ is a column vector of size (10×1). The boundary conditions stipulate that the vertical deflection be zero at node 1, 5 and 9. Boundary conditions are the known values of deflection and slope at specified values of x. Here the following boundary conditions are used for the exact analysis of the continuous beam.

At x = 0; y=0 At x= L; y= 0 At x= 2L; y=0

Thus reduced set of equations involving unknown nodal d.o.f. is obtained in matrix form as,

$\{f\}_{7 \times 1} = [k]_{7 \times 7} \{u\}_{7 \times 1}$ (5.8)

Solving the Equation 5.8, the nodal displacement is found out.
The experimental and numerical load-deflection curves obtained for the control beam, CB1 are illustrated in Figure 5.4.
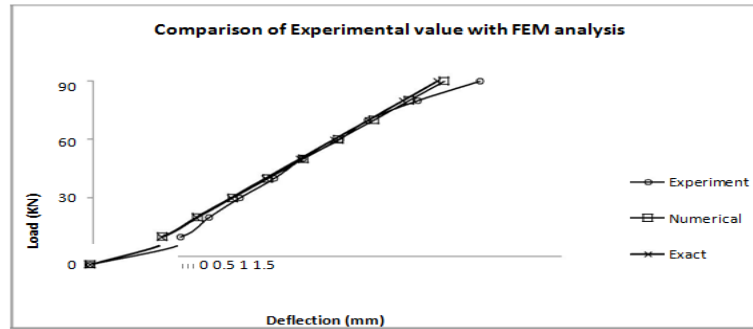
Figure 5.4 Comparison of Experimental value with Numerical and Exact analysis for CB1

The numerical and experimental results for the beam are shown in Figure 5.4. The trend of the loads varying with the deflection presents that the linear elastic state exits in the structure, when the loads are equivalent to about 90 KN.

VI. Conclusions

6.1 Conclusions

The present experimental study is carried out on the flexural behavior of reinforced concrete rectangular beams strengthened by GFRP sheets. Fourteen reinforced concrete (RC) beams weak in flexure having different set of reinforcement detailing are casted and tested. The beams were grouped into two series labeled S1 and S2. Each series had different longitudinal and transverse steel reinforcement ratios. From the test results and calculated strength values, the following conclusions are drawn:

1. The ultimate load carrying capacity of all the strengthen beams is higher when compared to the control beam.
2. The initial cracks in the strengthened beams are formed at higher load compared to control beam.
3. From series S1, beam SB9 which was strengthened by U-wrap and was anchored by using steel plate and bolt system, showed the highest ultimate load value of 415 KN. The percentage increase of the load capacity of SB9 was 61.92 %.
4. The load carrying capacity of beam SB6, which was strengthened by two layers of U-wrap of length 88 cm in positive moment zone and two layers of U-wrap of length 44 cm over first two layers, was 415 KN which was nearer to the load capacity of beam SB9. The percentage increase of load carrying capacity was 59.61 % , from which it can be concluded that applying FRP in the flexure zone is quite effective method to enhance the load carrying capacity.
5. TB3 beam from Series S2, which was strengthened by two layers of U-wrap in positive moment zone and two layers of U-wrap in flexure zone above first two layers, was having maximum ultimate load value of 326 KN, than the other strengthened beams of same category. The percentage increase of this beam was 63 % which was highest among all strengthened beams.
6. Using of steel bolt and plate system is an effective method of anchoring the FRP sheet to prevent the debonding failure.
7. Strengthening of continuous beam by providing U-wrap of FRP sheet is a new and effective way of enhancing the capacity of load carrying.
8. Flexural failure at the intermediate support section can be prevented by application of GFRP sheets.
9. In lower range of load values the deflection obtained using Finite Element models are in good agreement with the experimental results. For higher load values there is a deviation with the experimental results because linear FEM has been adopted.

6.2 Scope Of The Future Work

It promises a great scope for future studies. Following areas are considered for future research:

a. Experimental study of continuous beams with opening
b. Non linear analysis of RC continuous beam
c. FEM modeling of unanchored U-wrap
d. FEM modeling of anchored U-wrap

REFERENCES

[1]   ACI Committee 440, "Starte-of-the-art report on fiber reinforced plastic reinforcement for concrete structures", Report ACI 440R-96, USA: American Concrete Institute, 1996.
[2]   Aiello MA, Valente L, and Rizzo A, "Moment redistribution in continuous reinforced concrete beams strengthened

with carbon fiber-reinforced polymer laminates", Mechanicsof Composite Materials, vol. 43, pp. 453-466, 2007.

[3]   Aiello MA, and Ombres L, "Cracking and deformability analysis of reinforced concrete beams strengthened with externally bonded carbon fiber reinforced polymer sheet", ASCEJournal of Materials in Civil Engineering, vol. 16, No. 5, pp.292-399,2004.

[4]   Akbarzadeh H, and Maghsoudi AA, "Experimental and analytical investigation of reinforced high strength concrete continuous beams strengthened with fiber reinforced polymer", Materials and Design, vol. 31, pp. 1130-1147, 2010.

[5]   Arduini M, and Nanni A, "Behaviour of pre-cracked R. C. beams strengthened with carbon FRP sheets", ASCE Journal of Composites for Construction, vol. 1, No. 2, pp. 63-70, 1997.

[6]   Ashour AF, El-Refaie SA, and Garrity SW, "Flexural strengthening of RC continuous beams using CFRP laminates", Cement and Concrete Composites, vol. 26, pp. 765-775, 2003.

[7]   Bank LC, and Arora D, "Analysis of RC beams strengthened with mechanically fastened FRP (MF-FRP) strips", Composite Structures, vol. 79, pp. 180–191, 2006.

[8]   Bousselham A and Chaallal O, "Behavior of reinforced concrete T-beams strengthened in shear with carbon fiber reinforced polymer - an experimental study", ACI Structural Journal, vol. 103, pp. 339–347, 2006.

[9]   Brosens K, and Gemert D, "Anchoring stresses between concrete and carbon fiber reinforced laminates", Non-metallic (FRP) Reinforcement for Concrete Structures, Proc.of 3rd International Symposium, Sapporo, Japan, pp. 271–278, 1997.

[10]   Ceroni F, "Experimental performances of RC beams strengthened with FRP materials",Construction and Building Materials, vol. 24, pp. 1547-1559, 2010.

[11]   Chahrour A, and Soudki K, "Flexural response of reinforced concrete beams strengthened with end-anchored partially bonded carbon fiber-reinforced polymer strips", Journal ofComposites for Construction ASCE, vol. 9(2), pp. 170–177, 2005.

[12]   Concrete Society, "Design guidance for strengthening concrete structures using fibre composite materials", Report No. 55, 71p, 2000.

[13]   El-Refaie SA, Ashour AF, and Garrity SW, "CFRP strengthened continuous concrete beams", Proceedings of the ICE - Structures and Buildings, pp. 395 - 404, 2003.

[14]   El-Refaie SA, Ashour AF, and Garrity SW, "Sagging and hogging strengthening of continuous reinforced concrete beams using carbon fibre-reinforced polymer sheets", ACIStructural Journal, vol. 100, pp. 446-453, 2003.

[15]   El-Refaie SA, Ashour AF, and Garrity SW, "Sagging strengthening of continuous reinforced concrete beams using carbon fibre sheets", The 11th BCA Annual Conferenceon Higher Education and the Concrete Industry, Manchester, UK, pp. 281–292, 3–4 July2001.

[16]   El-Refaie SA, Ashour AF, and Garrity SW, "Strengthening of reinforced concrete continuous beams with CFRP composites", The International Conference on StructuralEngineering, Mechanics and Computation, Cape Town, South Africa, 2–4. , pp.1591–1598, April 2001.

[17]   El-Refaie SA, Ashour AF, and Garrity SW, "Tests of reinforced concrete continuous beams strengthened with carbon fibre sheets", The 10th BCA Annual Conference onHigher Education and the Concrete Industry, Birmingham, UK, pp. 187–198, Jun 2000.

[18]   Eshwar N, Nanni A, and Ibell TJ, "Performance of two anchor systems of externally bonded fiber-reinforced polymer laminates", ACI Materials Journal, vol. 105(1), pp. 72– 80, 2008.

[19]   Galati D, and De Lorenzis L, "Effect of construction details on the bond performance of NSM FRP bars in concrete", Advances in Structural Engineering, vol. 12(5), pp. 683– 700, 2009.

[20]   Garden HN, and Hollaway LC, "An experimental study of the influence of plate end anchorage of carbon fibre composite plates used to strengthen reinforced concrete beams", Composite Structures, vol. 42, pp. 175–188, 1998.

[21]   Garden HN, and Hollaway LC, "An experimental study of the influence of plate end anchorage of carbon fibre composite plates used to strengthen reinforced concrete beams", Composite Structures, vol. 42, pp. 175–188, 1998.

[22]   Grace NF, "Strengthening of negative moment region of reinforced concrete beams using carbon fiber- reinforced polymer strips", ACI Structural Journal, vol. 98, No. 3, pp. 347-358, 2001.

[23]   Grace NF, Sayed GA, and Saleh KR, "Strengthening of continuous beams using fibre reinforced polymer laminates", American Concrete Institute, Farmington Hills, Mich, pp. 647-657, 1999.

[24]   Grace NF, Wael R, and Sayed AA, "Innovative triaxailly braided ductile FRP fabric for strengthening structures", 7th International Symposium on Fiber Reinforce Polymer for Reinforced Concrete Structures, ACI, Kansas City, MO, 2005.

[25]   Grace NF, Abdel-Sayed G, Soliman AK, and Saleh KR, Strengthening of reinforced concrete beams using fibre reinforced polymer (FRP) laminates", ACI Structural Journal, vol. 96, No. 5, pp. 865-874, 1999.

[26]   Grace NF, Soliman AK, Abdel-Sayed G, and Saleh KR, "Strengthening of continuous beams using fibre reinforced polymer laminates", Proceedings of 4th InternationalSymposium on Fibre Reinforced Polymer Reinforcements for Reinforced Concrete Structures, SP-188, American Concrete Institute, Farmington Hills, Michigan, USA,pp.647-657, 1999.

[27]   Jumaat MZ, and Alam MA, "Experimental and numerical analysis of end anchored steel plate and CFRP laminate flexurally strengthened R. C. beams", International Journal ofPhysical Sciences, vol. 5, pp. 132-144, 2010.

[28]   Jumaat MZ, Rahman MM, and Rahman MA, "Review on bonding techniques of CFRP in strengthening concrete structures", International Journal of the Physical Sciences, vol. 6(15), pp. 3567-3575, 4 August. 2011.

[29]   Kadhim, "Effect of CFRP Sheet Length on the Behavior of HSC Continuous Beam", Journal of Thermoplastic composite materials, Vol. 00, 2011.

[30]   Khalifa A, and Nanni A, "Improving shear capacity of existing RC T-section beams using CFRP composites",

Cement and Concrete Composites, vol. 22, pp. 165–174, 2000.

[31] Khalifa A, Tumialan G, Nanni A, and Belarbi A, "Shear Strengthening of Continuous Reinforced Beams Using Externally Bonded Carbon Fiber Reinforced Polymer Sheets", In: Fourth International Symposium on Fiber Reinforced Polymer Reinforcement forReinforced Concrete Structures, Baltimore, MD, American Concrete Institute, pp. 995–1008, November 1999.

[32] Lamanna AJ, Bank LC, and Scott DW, "Flexural strengthening of reinforced concrete beams using fasteners and fiber-reinforced polymer strips", ACI Structural Journal, vol. 98(3), pp. 368–76, 2001.

[33] Lee TK, and Al-Mahaidi R, "An experimental investigation on shear behaviour of RC T-beams strengthened with CFRP using photogrammetry", Composite Structures, vol. 82, pp. 185–193, 2008.

[34] Leung CKY, and Cao Q, "Development of strain hardening permanent formwork for durable concrete structures", Materials and Structures, vol. 43(7), pp. 993–1007, 2009.

[35] Leung CKY, "Delamination failure in concrete beams retrofitted with a bonded plate",Journal of Materials in Civil Engineering, vol. 13, pp. 106–113, 2001.

[36] Leung CKY, "FRP debonding from a concrete substrate: Some recent findings against conventional belief", Cement and Concrete Composites, vol. 28, pp. 742–748, 2006.

[37] Maghsoudi AA, and Bengar H, "Moment redistribution and ductility of RHSC continuous beams strengthened with CFRP", Turkish Journal of Engineering and EnvironmentalSciences, vol. 33, pp. 45-59, 2009.

[38] Micelli F, Anniah RH, and Nanni A, "Strengthening of short shear span reinforced concrete T joists with fiber reinforced plastic composites", Journal of Composites forConstruction, vol. 6, pp. 264–271, 2002.

[39] Nguyen DM, Chan TK, and Cheong HK, "Brittle failure and bond development length of CFRP-concrete beams", Journal of Composites for Construction, vol. 5(1), pp. 12–17,2001.

[40] Niemitz CW, James R, and Berña SF, "Experimental behavior of carbon fiber-reinforced polymer (CFRP) sheets attached to concrete surfaces using CFRP anchors", Journal ofComposites for Construction, vol. 12(2), pp. 185–194, 2010.

[41] Obaidat YT, Susanne H, Ola D, Ghazi A, Yahia A, "Retrofitting of reinforced concrete beams using composite laminates", Construction and Building Materials, vol. 25, pp. 591-597, 2010.

[42] Oehlers DJ, Liu IST, and Seracino R, "Shear deformation debonding of adhesively bonded plates" Proc. Institution of Civil Engineers, vol. 158(1), pp. 77–84, 2005.

[43] Orton, SL, Jirsa JO, and Beyrak O, "Design considerations of carbon fiber anchors."Journal of Composites for Construction, vol. 12(6), pp. 608–616, 2008.

[44] Pan JL, and Leung CKY, "Effect of concrete composition on FRP/concrete bond capacity." Journal of Composites for Construction, vol. 11(6), pp. 611–618, 2007.

[45] Rahimi H, and Hutchinson A, "Concrete beams strengthened with externally bonded FRP plates." Journal of Composites for Construction, vol. 5(1), pp. 44–56, 2001.

[46] Ritchie PA, Thomas DA, Lu LW, and Connelly GM, "External reinforcement of concrete beams using fiber reinforced plastic", ACI Structural Journal, vol. 88(4), pp. 490– 500,1991.

[47] Smith ST, and Teng JG, "Debonding failures in FRP-plated RC Beams with or without U strip end anchorage", Proc. FRP Composites in Civil Engineering, vol. 1, pp. 607–615, 2001.

[48] Panda KC, Bhattacharyya SK, and Barai SV, "Shear behaviour of reinforced concrete T-beams with U-bonded glass fibre reinforced plastic sheet", Indian Concrete Journal, vol. 84, pp. 61–71, 2010.

[49] Riyadh A, "Coupled flexural retrofitting of RC beams using CFRP straps", CompositeStructures, vol. 75, pp. 457-464, 2006.

[50] Ross CA, Jerome DM, Tedesco JW, and Hughes ML, "Strengthening of reinforced concrete beams with externally bonded composite laminates", ACI Structural Journal, vol. 96. No. 2, pp. 65-71, 1999.

[51] Sebastian WM, "Significance of mid-span de-bonding failure in FRP-plated concrete beams", ASCE Journal of Structural Engineering, vol. 127, No. 7, pp.792-798, 2001.

[52] Sheikh SA, "Performance of concrete structures retrofitted with fibre reinforced polymers", Engineering Structures, vol. 24, pp. 869-879, 2002.

[53] Smith ST, and Teng JG, "FRP-strengthened RC beams I: Review of debonding strength models", Engineering Structures, vol. 24, No. 4, pp. 385-395, 2002.

[54] Spadea G, Bencardino F, and Swamy RN, "Structural behaviour of composite RC beams with externally bonded CFRP", Journal of Composites for Construction, ASCE, pp. 132– 7, 1998.

[55] Teng JG, Smith ST, Yao J, and Chen JF, "Intermediate crack-induced debonding in RC beams and slabs", Construcion and Building Materials, vol. 17(6–7), pp. 447–462, 2003.

[56] Yang ZJ, Chen JF, and Proverbs D, "Finite element modelling of concrete cover separation failure in FRP plated R. C. beams", Construction and Building Materials, vol. 17, No.1, pp. 3-13, 2003.

[57] Yao J, and Teng JG, "Plate end debonding in FRP-plated RC beams—I: Experiments",Engineering Structures, vol. 29(10), pp. 2457–2471, 2007.

[58] Yao J, Teng, JG, and Lam L, "Experimental study on intermediate crack debonding in FRP-strengthened RC flexural members", Advances in Structural Engineering, vol. 8(4), pp. 365–396, 2005.